Boundary Value Problems: Numerical (Approximate) Methods

6

Although this may seem a paradox, all exact science is dominated by the idea of approximation

Bertrand Russell, (1872–1970),
philosopher, mathematician, historian

6.1 Introduction

In **Chapter 5**, we discussed analytic methods of solution for electrostatic problems. The most outstanding feature of these methods was that the solution was exact and in the form of a mathematical relation. On the other hand, only certain classes of problems could be solved. In the case of the method of images, the question was one of finding the correct system of images, a requirement that meant, almost always, that a constant potential surface exists or can be stipulated. If this conducting surface is very complex, the condition of constant potential on the surface may not be as easy to satisfy. Similarly, separation of variable, while certainly valid in general, is often difficult to apply because of the need to satisfy complex boundary conditions. If the boundaries of the problem are not parallel to coordinates, it is next to impossible to find the constants required for solution. Even for the simple planar geometries discussed in **Chapter 5**, the solution required considerable skill. Furthermore, precious little was said about solution of Poisson's equation. For another example of the difficulty in analytic solutions, consider **Figure 6.1**, which shows a simple parallel plate capacitor. Suppose we need to calculate its capacitance. One method we used before is to assume that the plates are very close to each other, neglect fringing, and use the formula for the parallel plate capacitor. In **Figure 6.1a**, the distance between the plates is very small, and the capacitance may be approximated as $C = \varepsilon A/d$ [F]. **Figure 6.1b** shows the same two plates, but now the plates are much farther apart, perhaps because our design requires that this capacitor withstand high voltages. Here, we cannot neglect fringing, and, therefore, the use of the formula for parallel plate capacitors is incorrect. How can we solve this problem? It seems that none of the methods of the previous chapters applies here. Yet, this type of problem is quite common. Other examples are the voltage and fields of power lines in the presence of conducting objects (such as transformers, towers, buildings, etc.), field distributions between nonparallel surfaces, and many others. Although, in some cases, assumptions can be made to simplify the problem, this is not always possible and we are faced with the need to solve problems for which analytic methods cannot be used.

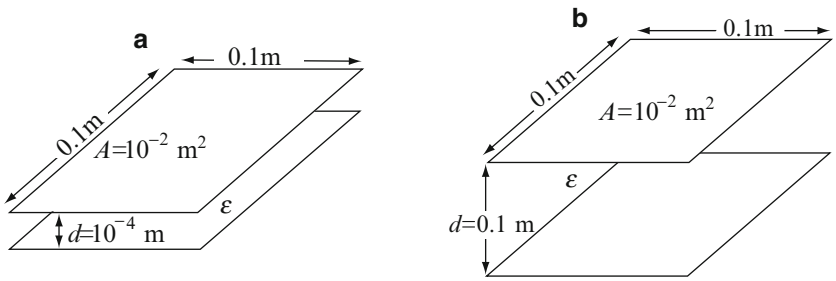

Figure 6.1 (**a**) Parallel plate capacitor for which fringing fields can be neglected. (**b**) d is large and fringing cannot be neglected

There are a number of numerical methods that can be used when analytic methods fail. These methods, some of which are very old and others quite new, are all based on availability of computers to solve the field equations. Some of the more

N. Ida, *Engineering Electromagnetics*, DOI 10.1007/978-3-319-07806-9_6,

common numerical techniques will be described next. We will first describe the general idea of a numerical method and then discuss in detail three representative methods for numerical solution of electrostatic problems.

Before we plunge into numerical methods of solutions, it is well to reiterate that, in a way, the only reason for doing so is our inability to solve the problem analytically; that is, the goal should always be an analytic, closed-form solution. Even when numerical solutions are pursued, and they are pursued quite often, analytic methods are still important as a means of checking numerical solutions.

6.1.1 A Note on Computer Programs

Numerical methods require computers, and computers require computer programs. The examples solved in this chapter as well as many of the problems at the end of the chapter use computer programs for solutions. The programs required to solve the various examples are available (in Matlab) from http://extras.springer.com/2014/978-3-319-07806-9 and can be downloaded when required. The site also lists the various input and output files referred to in the text as well as an information file with explanations. It is recommended that these programs and data files be downloaded before any attempt at understanding the examples given in this chapter is undertaken. The site contains other programs that may be useful. These computer programs were written in the simplest possible way with a minimum of constructs. To keep things simple and easily understandable, the programs were specifically written for the examples given. Because of that, they are not general. However, they can serve as the basis for more general programs and, in particular, may be adapted for solution of the end-of-chapter problems. Most of the checks usually found in programs (such as limits on arrays, correctness of values, and the like) have been taken out to keep the programs short. Thus, the user should be careful with the data or incorrect results will be obtained. To aid in this task, the input data for the given results is also included with the program and a free-format primitive interrogative input is included in each program. Programs are referred in the text by name.

6.2 The General Idea of Numerical Solutions

What is then a numerical method? Quite simply, any method that solves a class of problems, based on discretization of the continuum and approximation of the solution variables in some systematic and, preferably, simple way. An analogy is in order here: Suppose you need to make a soccer ball out of leather. A perfect ball made out of a single piece of leather is impossible to make; yet, a perfect ball is what we want—that is the analytic solution. Instead, we might proceed to form two half-spheres by, say, pressing and stretching the leather in the same way shoe tips are made. This is one possible approximation, but it is not a simple approximation because it requires complicated machinery. Instead, we could choose small, simple patches of some defined shape, all planar, and stitched together. One example is the triangular pattern. Another is a hexagonal patch. A third (the way soccer balls are actually made) is a combination of pentagonal (black) and hexagonal (white) patches. The ball has 32 patches sewn together, to form a 32-faceted volume that approximates a sphere. Any of these approximations is valid, although, in this case, the pentagonal/hexagonal approximation is used by convention. The approximation process is shown in **Figure 6.2**.

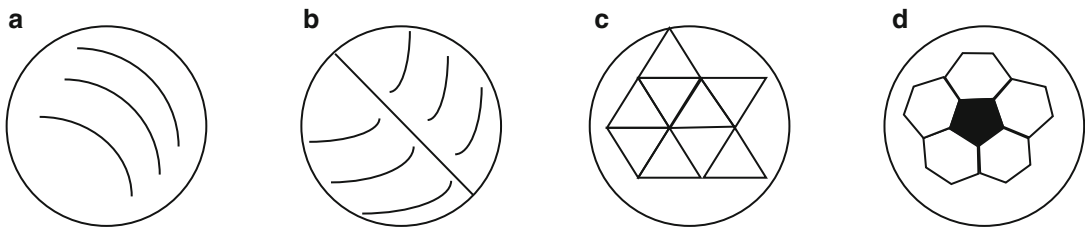

Figure 6.2 The approximation process. (**a**) A perfect ball. (**b**) A ball made of two half-spheres. (**c**) A ball made of triangular patches. (**d**) A soccer ball made of hexagonal and pentagonal patches

The above process is the essence of any approximation method. The whole process is based on the premise that if the approximation is not good enough (such as using 32 patches for a soccer ball), we can increase the number of patches while decreasing their size as much as we wish. In the limit, the number of patches tends to infinity, with their size tending to zero; that is, the patches are reduced to points and the approximation becomes "exact."

A similar example is shown in **Figure 6.3a**. A general surface contains a nonuniform charge density and we need to calculate the total charge or the electric potential at a point in space. We know how to solve this problem analytically: All we have to do is integrate the surface charge density over the surface. In practice, however, unless the surface representation is simple, we cannot perform the integration. An approximate solution may be found by dividing the surface into any number of small subdomains and assuming each subdomain has a constant but different charge density, depending on the location of the subdomain (**Figure 6.3b**). If the subdomains are small, and we are free to make them as small as we wish, the total charge of each subdomain may be taken as a point charge at the center of the subdomain and the problem is solved as if we had as many point charges as we have subdomains, with the point charges located at the center of the subdomains. Now, of course, the problem is simple, except for the fact that we have many, perhaps many thousands of points to evaluate, hence the need for a computer, even for the simple integration described here.

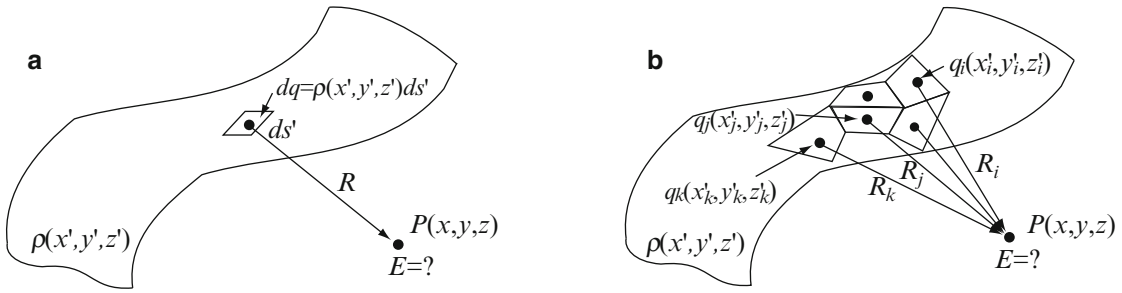

Figure 6.3 (**a**) Nonuniform charge distribution on a complex surface. (**b**) Division of the surface into patches, each with a different but constant charge density

6.3 The Finite Difference Method: Solution to the Laplace and Poisson Equations

The finite difference method is the oldest of the numerical methods; its origins have been traced to Gauss. However, as we shall see shortly, it only really came into widespread use with the advent of the computer because, whereas the calculations necessary are very simple, there are a large number of calculations that need to be performed. The finite difference method consists of replacing the partial derivatives in the partial differential equation describing the physical process by an algebraic approximation based on simple relations between the values of the function we need to evaluate. Since these relations are in the form of differences between values of the function, and these values are at small but finite distances from each other, the method is called a ***finite difference method***.

We will present the finite difference method for Laplace's and Poisson's equations based on the definition of the derivative. This is simple and intuitive, and most importantly, it shows the physical interpretation of the approximations involved. The formal definition of the finite difference method is based on truncated Taylor series. These have the advantage that they allow the definition of approximations to any derivative and also, by truncating the series at different locations, different approximation errors may be allowed. However, for the type of equations we need to solve here (and, in fact, throughout this book), only first- and second-order derivatives are needed. Therefore, we first define the general approximation for first-order derivatives. From this approximation, we then derive an approximation to second-order derivatives and then apply these to the solution of Laplace's and Poisson's equations.

6.3.1 The Finite Difference Approximation: First-Order Derivative

The approximation to a first-order derivative can be found in the definition of the derivative itself. Consider **Figure 6.4a**, where a general function of a single variable is shown. The function is shown as a continuous function, but it may also be a sequence of points such as may be obtained from measurements. The derivative $f'(x) = df/dx$ at a point x_i is the tangent to the curve at this point (line f'). An approximation to the derivative can be found by taking two points, say on both sides of the point x_i, and passing a straight line through them. If the two points are chosen to be equally spaced about the point x_i, as in **Figure 6.4a** (line f_i'), the following expression for the slope of the line is obtained:

$$\boxed{\frac{df(x_i)}{dx} \approx \frac{f(x_i + \Delta x) - f(x_i - \Delta x)}{2\Delta x}} \tag{6.1}$$

Because the derivative is evaluated using two symmetric points around x_i, this expression is called a ***central difference formula*** and is immediately recognized as the definition of the derivative if we allow Δx to tend to zero. This is a valid approximation to the derivative, but it is not the only possible approximation. Another valid approximation (slope) at point x_i is (line f_2')

$$\boxed{f_2' = \frac{df(x_i)}{dx} \approx \frac{f(x_i + \Delta x) - f(x_i)}{\Delta x}} \tag{6.2}$$

This is called a ***forward difference formula*** because it uses the point x_i and points ahead of it ($x_i + \Delta x$). A third approximation is that of line f_3':

$$\boxed{f_3' = \frac{df(x_i)}{dx} \approx \frac{f(x_i) - f(x_i - \Delta x)}{\Delta x}} \tag{6.3}$$

This is called a ***backward difference formula*** because it uses the point x_i and points behind it ($x_i - \Delta x$). The three approximations are not identical, and, therefore, one may be a better approximation than the other, but all three are valid because in the limit, as Δx approaches zero, all three lead to the correct slope of the function at point x_i.

6.3.2 The Finite Difference Approximation: Second-Order Derivative

An approximation to the second-order derivative may be obtained from the first-order derivatives using the method of the previous section. Suppose that we used the formula in **Eq. (6.3)** to calculate the first-order derivative at all points of the function in **Figure 6.4a**. The result is the function in **Figure 6.4b**. This function is drawn as a continuous function to indicate that the number of points can be as large as necessary, Δx can be as small as necessary, and, therefore, the function describing the derivative can be as close to a continuous function as is practical. Now, we start with the function in **Figure 6.4b** and calculate the first-order derivative at a point x_i using **Eq. (6.2)**. This gives

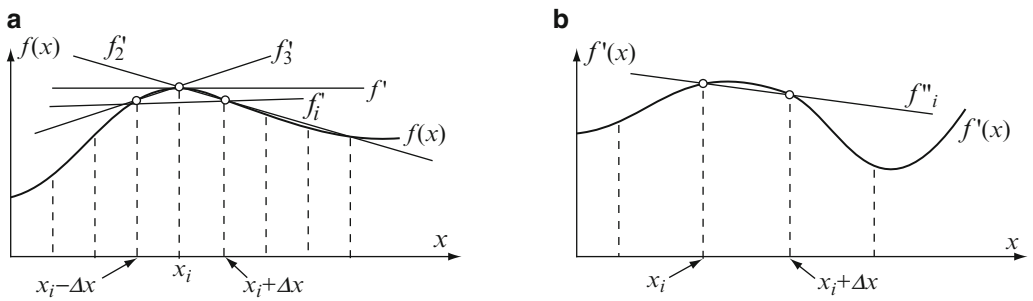

Figure 6.4 (**a**) Exact first derivative f' and approximations to the first derivative at point x_i. (**b**) Approximation to the second derivative at point x_i

$$f''(x_i) = \frac{df'(x_i)}{dx} \approx \frac{f'(x_i + \Delta x) - f'(x_i)}{\Delta x} \tag{6.4}$$

From **Figure 6.4a** the derivatives $f'(x_i + \Delta x)$ and $f'(x_i)$ are given in terms of the original function [using **Eq. (6.3)**] as

$$f'(x_i + \Delta x) = \frac{f(x_i + \Delta x) - f(x_i)}{\Delta x} \quad \text{and} \quad f(x_i) = \frac{f(x_i) - f'(x_i - \Delta x)}{\Delta x} \tag{6.5}$$

Substitution of these two approximations into **Eq. (6.4)** gives

$$\frac{d^2f(x_i)}{dx^2} = \frac{df'(x_i)}{dx} \approx \frac{1}{\Delta x}\left[\frac{f(x_i+\Delta x)-f(x_i)}{\Delta x} - \frac{f(x_i)-f(x_i-\Delta x)}{\Delta x}\right] \tag{6.6}$$

Collecting terms, we get the approximation for the second-order derivative:

$$\frac{d^2f(x_i)}{dx^2} \approx \frac{f(x_i+\Delta x)-2f(x_i)+f(x_i-\Delta x)}{(\Delta x)^2} \tag{6.7}$$

To derive this equation, we used **Eqs. (6.2)** and **(6.3)**, but other possibilities exist (see **Exercise 6.1**).
Before continuing, we rewrite **Eq. (6.7)** in short-form notation by denoting $x_i + \Delta x$ as x_{i+1}, $x_i - \Delta x$ as x_{i-1}, and Δx as h:

$$\boxed{\frac{d^2f_i}{dx^2} \approx \frac{f_{i+1}-2f_i+f_{i-1}}{h^2}} \tag{6.8}$$

If the function f were a function of the y or z variables, the approximation in each case would be

$$\frac{d^2f(y)}{dy^2} \approx \frac{f_{j+1}-2f_j+f_{j-1}}{(\Delta y)^2} \quad \text{and} \quad \frac{d^2f(z)}{dz^2} \approx \frac{f_{k+1}-2f_k+f_{k-1}}{(\Delta z)^2} \tag{6.9}$$

The last step in our approximation is to assume that the approximation to the second-order ordinary derivative above is also a good approximation to the second-order partial derivative.

The above functions were each dependent on one variable alone. To define the second-order derivative of a function of two variables, we assume that the function $f(x,y)$ is defined over a surface S **(Figure 6.5)** and its values are known everywhere on the surface. For simplicity, we will also assume that $\Delta x = \Delta y = h$. Now, we can write the following using **Figure 6.5** and **Eq. (6.8)**:

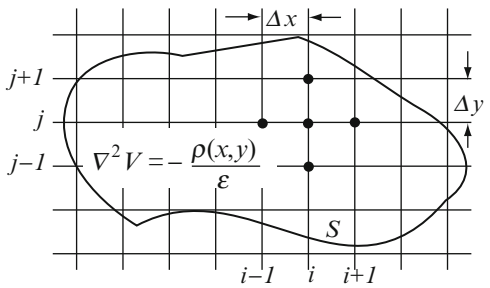

Figure 6.5 A surface divided into a grid (or mesh) over which the function $f(x, y)$ is approximated using finite differences

$$\frac{\partial^2f(x,y)}{\partial x^2} \approx \frac{f_{i-1,j}-2f_{i,j}+f_{i+1,j}}{h^2} \quad \text{and} \quad \frac{\partial^2f(x,y)}{\partial y^2} \approx \frac{f_{i,j-1}-2f_{i,j}+f_{i,j+1}}{h^2} \tag{6.10}$$

Combining the two, we get an expression for the two-dimensional Laplacian:

$$\frac{\partial^2f(x,y)}{\partial x^2} + \frac{\partial^2f(x,y)}{\partial y^2} \approx \frac{f_{i-1,j}-2f_{i,j}+f_{i+1,j}}{h^2} + \frac{f_{i,j-1}-2f_{i,j}+f_{i,j+1}}{h^2} \tag{6.11}$$

or, combining terms,

$$\boxed{\frac{\partial^2f(x,y)}{\partial x^2} + \frac{\partial^2f(x,y)}{\partial y^2} \approx \frac{f_{i-1,j}+f_{i+1,j}+f_{i,j-1}+f_{i,j+1}-4f_{i,j}}{h^2}} \tag{6.12}$$

The Laplacian in three dimensions is obtained similarly. All we need to do is add the partial derivative with respect to z. The form of the derivative is identical to that in **Eq. (6.12)**, but now there are three indices, one in each dimension. Assuming that $\Delta x = \Delta y = \Delta z = h$ gives (see **Exercises 6.2** and **6.3**)

$$\boxed{\begin{aligned}&\frac{\partial^2 f(x,y,z)}{\partial x^2}+\frac{\partial^2 f(x,y,z)}{\partial y^2}+\frac{\partial^2 f(x,y,z)}{\partial z^2}\\&\quad\approx\frac{f_{i-1,j,k}+f_{i+1,j,k}+f_{i,j-1,k}+f_{i,j+1,k}+f_{i,j,k-1}+f_{i,j,k+1}-6f_{i,j,k}}{h^2}\end{aligned}} \tag{6.13}$$

The approximation in three dimensions is just as simple as in two dimensions. However, because three-dimensional problems are more difficult to visualize and the bookkeeping tasks on the various indices are more complex, most (but not all) of the problems solved here are two-dimensional applications.

We are now in a position to use these approximations to find solutions to electrostatic field problems. First, we define the approximation in terms of the scalar potential V for Laplace's equation in two dimensions. In terms of the electric potential, this is [from **Eq. (6.12)**]

$$\frac{\partial^2 V(x,y)}{\partial x^2}+\frac{\partial^2 V(x,y)}{\partial y^2}\approx\frac{V_{i-1,j}+V_{i+1,j}+V_{i,j-1}+V_{i,j+1}-4V_{i,j}}{h^2}=0 \tag{6.14}$$

or, multiplying both sides by $h^2 = (\Delta x)^2$, the approximation for the potential at point (i,j) is

$$\boxed{V_{i,j}=\frac{V_{i-1,j}+V_{i+1,j}+V_{i,j-1}+V_{i,j+1}}{4}\quad[\text{V}]} \tag{6.15}$$

This approximation is independent of h. The approximation to Poisson's equation is [see **Eq. (5.5)**]

$$\frac{V_{i-1,j}+V_{i+1,j}+V_{i,j-1}+V_{i,j+1}-4V_{i,j}}{h^2}=-\frac{\rho(x,y)}{\varepsilon(x,y)}\quad[\text{V}] \tag{6.16}$$

where $\rho(x,y)$ is the surface charge density (if any). From this, the approximation for the potential at point (i,j) is

$$\boxed{V_{i,j}=\frac{V_{i-1,j}+V_{i+1,j}+V_{i,j-1}+V_{i,j+1}}{4}+\frac{h^2\rho_{i,j}}{4\varepsilon_{i,j}}\quad[\text{V}]} \tag{6.17}$$

Exercise 6.1 Find an approximation to the second-order derivative as follows:

(a) Use **Eq. (6.1)** alone, noting that the derivative is approximated using two points symmetric about point x_i.
(b) Use **Eq. (6.2)** alone, noting that the derivative at point x_i is approximated using points x_i and x_{i+1}.
(c) Why are these formulas less attractive than the one obtained in **Eq. (6.7)**?

Answer

(a) $\dfrac{d^2 f(x_i)}{dx^2}\approx\dfrac{f_{i+2}-2f_i+f_{i-2}}{(2\Delta x)^2}$. **(b)** $\dfrac{d^2 f(x_i)}{dx^2}\approx\dfrac{f_{i+2}-2f_{i+1}+f_i}{(\Delta x)^2}$.

(c) The approximation in **(a)** requires five points (even though $f_i(x_i + \Delta x)$ and $f_i(x_i - \Delta x)$ are not explicitly used), whereas the approximation in **(b)** is not symmetric about the calculation point. Both of these approximations, although valid, lead to reduced accuracy.

6.3.3 Implementation

Now that we have the approximations for Poisson's and Laplace's equations, we need to define the solution procedure. To do so, we use the example in **Figure 6.6**. It consists of a box, with three sides connected to zero potential and the fourth set to a constant potential $V_0 = 10$ V. The third dimension of the box (perpendicular to the page) is infinite, making this a two-dimensional

problem. This particular problem is described by Laplace's equation; therefore, we will use the approximation in **Eq. (6.14)** or **(6.15)**, depending on the method we adopt for solution. This particular problem has an analytic solution, obtained by separation of variables (see **Section 5.4.4.1** and **Problem 5.30**), so that the finite difference solution may be verified.

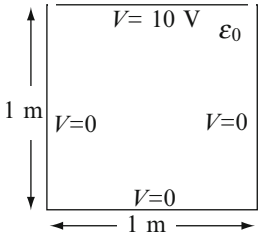

Figure 6.6 A simple geometry used to demonstrate finite difference solutions for electrostatic fields (Laplace's equation)

We have now two ways to solve the problem: The first is called an ***implicit method*** in which all potential values inside the box are taken as unknown values. Using the approximation in **Eq. (6.14)**, we write an equation at each internal node, relating the unknown potential at the node with the unknown potentials at the neighboring nodes. This results in a system of equations in N unknowns which is solved to obtain the unknown potentials. The second method is an ***explicit method***. In this method, all potential values are assumed to be known. Since we do not know the potentials at the internal nodes, we guess their value and then proceed to calculate new, updated values at the nodes, based on the known values at the nodes around them. To do so, we assume that the potential at node (i,j) is not known but all other nodes are known and use **Eq. (6.15)**. This process results in an updated value at node (i,j). The process is repeated iteratively until the solution at all nodes does not change or changes very little. The resulting potentials are the "correct" potentials at the nodes.

In general, explicit methods are preferred in finite difference problems. Their main advantage is in that there is no need to create, store, and solve a large system of equations. Although explicit methods cannot always be applied, they are applicable to all electrostatic problems we will encounter as well as many others. Both methods are shown here, starting with the implicit solution.

6.3.3.1 Implicit Solution

Implicit finite difference solution to an electrostatic problem is performed in six basic steps:

Step 1 First, we define a solution domain. This is the domain in which the potential must be obtained and is shown in **Figure 6.6** for a particular example. In this case, the solution domain is clearly defined by the actual, conducting boundaries, but in other applications, the boundaries must be decided upon based on the physical configuration. An example of this need to define boundaries is given in **Example 6.2**.

Step 2 Next, we define the boundary conditions of the problem. Remember that without boundary conditions, we cannot obtain a particular solution to a differential equation. This is true in analytic solutions and in numerical solutions. The boundary conditions are also shown in **Figure 6.6** as the known potentials on the surfaces of the box. This type of boundary condition is known as a ***Dirichlet boundary condition***.

Step 3 The solution domain is divided into a grid such that $\Delta x = \Delta y$. The intersections of the grid lines define the nodes of the solution domain at which the potentials will be calculated. The nodes are marked with the appropriate i, j indices as shown in **Figure 6.7a** for one choice of the grid. To simplify the discussion, we only divided the box into a 5×5 grid, with a total of 36 nodes. Of these, 16 are internal to the boundary and 20 are on the boundary. The 20 potentials on the boundary are known, whereas the 16 inside the solution domain are not known and must be evaluated.

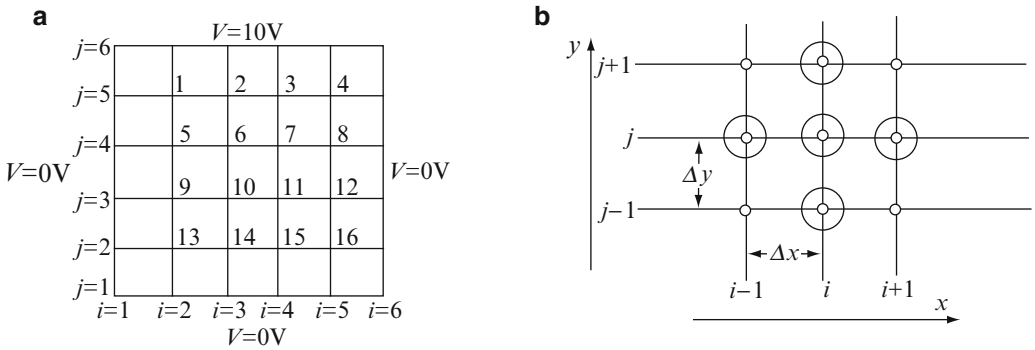

Figure 6.7 (**a**) Finite difference grid and node numbering for internal nodes. (**b**) Notation used for finite difference approximation. The five nodes marked are those used to approximate the Laplacian at point (i,j)

Step 4 The approximation in **Eq. (6.14)** is applied at each of the internal nodes. The approximation uses five points, including the node at which the potential is evaluated as shown in **Figure 6.7b**. The resulting "stencil" is applied at each point of the grid. This results in 16 equations in 16 unknowns as follows.

At a general node, for which the stencil does not include a border node such as node 11, we get: At node 11: $i = 4, j = 3$:

$$-4V_{4,3} + V_{3,3} + V_{5,3} + V_{4,2} + V_{4,4} = 0 \quad \rightarrow \quad 4V_{11} - V_{10} - V_{12} - V_{15} - V_7 = 0$$

where the final expression is written in terms of node numbers rather than the indices i, j. Similar expressions are obtained for nodes 6, 7, and 10.

At a node near the boundary for which the stencil includes a boundary node, we get: At node 2: $i = 3, j = 5$:

$$-4V_{3,5} + V_{2,5} + V_{4,5} + V_{3,4} + V_{3,6} = 0 \quad \rightarrow \quad 4V_2 - V_1 - V_3 - V_6 - 10 = 0$$

where the boundary value for the node at index $i = 3, j = 6$ was substituted as a boundary condition. Similar expressions are obtained for nodes 3, 5, 8, 9, 12, 14, and 15.

At a corner node such as node 4, two of the points in the stencil are on the boundary. The two values at the boundary nodes are substituted in the appropriate index locations: At node 4: $i = 5, j = 5$:

$$-4V_{5,5} + V_{4,5} + V_{6,5} + V_{5,4} + V_{5,6} = 0 \quad \rightarrow \quad 4V_4 - V_3 - 0 - V_8 - 10 = 0$$

Similar expressions are obtained for nodes 1, 13, and 16. After applying the approximation, we obtain a system of 16 equations in 16 unknowns. We write these relations with the free value on the right-hand side. For example, the equations for nodes 11, 2, and 4 become

$$\begin{aligned} 4V_{11} - V_{10} - V_{12} - V_{15} - V_7 &= 0, \\ 4V_2 - V_1 - V_3 - V_6 &= 10, \\ 4V_4 - V_3 - V_8 &= 10 \end{aligned}$$

Performing identical operations for all other interior nodes, and writing the resulting 16 equations into a matrix form, we get

$$\begin{bmatrix} 4 & -1 & 0 & 0 & -1 & 0 & 0 & 0 & 0 & 0 & 0 & 0 & 0 & 0 & 0 & 0 \\ -1 & 4 & -1 & 0 & 0 & -1 & 0 & 0 & 0 & 0 & 0 & 0 & 0 & 0 & 0 & 0 \\ 0 & -1 & 4 & -1 & 0 & 0 & -1 & 0 & 0 & 0 & 0 & 0 & 0 & 0 & 0 & 0 \\ 0 & 0 & -1 & 4 & 0 & 0 & 0 & -1 & 0 & 0 & 0 & 0 & 0 & 0 & 0 & 0 \\ -1 & 0 & 0 & 0 & 4 & -1 & 0 & 0 & -1 & 0 & 0 & 0 & 0 & 0 & 0 & 0 \\ 0 & -1 & 0 & 0 & -1 & 4 & -1 & 0 & 0 & -1 & 0 & 0 & 0 & 0 & 0 & 0 \\ 0 & 0 & -1 & 0 & 0 & -1 & 4 & -1 & 0 & 0 & -1 & 0 & 0 & 0 & 0 & 0 \\ 0 & 0 & 0 & -1 & 0 & 0 & -1 & 4 & 0 & 0 & 0 & -1 & 0 & 0 & 0 & 0 \\ 0 & 0 & 0 & 0 & -1 & 0 & 0 & -1 & 4 & 0 & 0 & 0 & -1 & 0 & 0 & 0 \\ 0 & 0 & 0 & 0 & 0 & -1 & 0 & 0 & -1 & 4 & -1 & 0 & 0 & -1 & 0 & 0 \\ 0 & 0 & 0 & 0 & 0 & 0 & -1 & 0 & 0 & -1 & 4 & -1 & 0 & 0 & -1 & 0 \\ 0 & 0 & 0 & 0 & 0 & 0 & 0 & -1 & 0 & 0 & -1 & 4 & -1 & 0 & 0 & -1 \\ 0 & 0 & 0 & 0 & 0 & 0 & 0 & 0 & -1 & 0 & 0 & 0 & 4 & -1 & 0 & 0 \\ 0 & 0 & 0 & 0 & 0 & 0 & 0 & 0 & 0 & -1 & 0 & 0 & -1 & 4 & -1 & 0 \\ 0 & 0 & 0 & 0 & 0 & 0 & 0 & 0 & 0 & 0 & -1 & 0 & 0 & -1 & 4 & -1 \\ 0 & 0 & 0 & 0 & 0 & 0 & 0 & 0 & 0 & 0 & 0 & -1 & 0 & 0 & -1 & 4 \end{bmatrix} \begin{bmatrix} V_1 \\ V_2 \\ V_3 \\ V_4 \\ V_5 \\ V_6 \\ V_7 \\ V_8 \\ V_9 \\ V_{10} \\ V_{11} \\ V_{12} \\ V_{13} \\ V_{14} \\ V_{15} \\ V_{16} \end{bmatrix} = \begin{bmatrix} 10 \\ 10 \\ 10 \\ 10 \\ 0 \\ 0 \\ 0 \\ 0 \\ 0 \\ 0 \\ 0 \\ 0 \\ 0 \\ 0 \\ 0 \\ 0 \end{bmatrix} \tag{6.18}$$

This matrix is unique to finite difference methods. The diagonal in each row is 4 (for three-dimensional applications it is 6 and for one-dimensional applications it is always 2). The off-diagonal terms are -1 at the locations of the outer points of the finite difference stencil and zero elsewhere. The location of the nonzero, off-diagonal terms depends on the numbering sequence adopted. The right-hand side contains all free terms. Because of this very simple structure, the matrix can be built directly from the finite difference grid without the need to construct the equations explicitly.

Step 5 The potentials are obtained by solving the system of equations in **Eq. (6.18)**. Any method of solution may be employed. For example, we may use the Gaussian elimination method, Gauss–Seidel method, or any other solution method applicable to the solution of linear systems of equations. Computational software tools may also be used.

Program **fdmimp.m** assembles and solves the system of equations using Gaussian elimination. The program is rather general in that it can be applied to other finite difference problems but is simple enough to be understood. The potentials V_1 through V_{16} obtained from the program are shown in **Figure 6.8**, in the same sequence as the nodes are numbered in **Figure 6.7a**, together with the boundary values.

10.0	10.0	10.0	10.0	10.0	10.0
0.0	4.5455	5.9470	5.9470	4.5455	0.0
0.0	**2.2348**	3.2955	3.2995	2.2348	0.0
0.0	1.0985	1.7045	1.7045	1.0985	0.0
0.0	0.4545	0.7197	0.7197	0.4545	0.0
0.0	0.0	0.0	0.0	0.0	0.0

Figure 6.8 Potentials at the interior and boundary nodes in **Figure 6.7a**. The solution at node #5 is emphasized

Step 6 The final step in the solution of a numerical method may be called a "data processing" step and includes any additional calculations such as calculation of electric fields from potentials, display of data, and interpretation of results. One way to present the results is given in **Figure 6.8**, where the potentials at the nodal points are shown as a list. **Figure 6.9a** shows a different form of the solution by showing equal potential lines in a plot. This type of representation is useful in design because it shows where the potential is high and where the gradients are high (distance between lines is small). **Figure 6.9b** shows the same result in a three-dimensional plot. Various types of plots, including these shown here, are easily obtained with commercially available graphing software.[1] In the present problem, the density is highest at and around the upper left and upper right corners, where the potential changes from 10 V to 0 V in a very short distance. In other cases, the solution might mean the capacitance of a device, breakdown voltage in a gap, or the electric field intensity in the solution domain or at a point. The latter is calculated by employing the finite difference method as an approximation to the derivative and calculating the terms of the gradient in the potential as we shall see in **Example 6.1**.

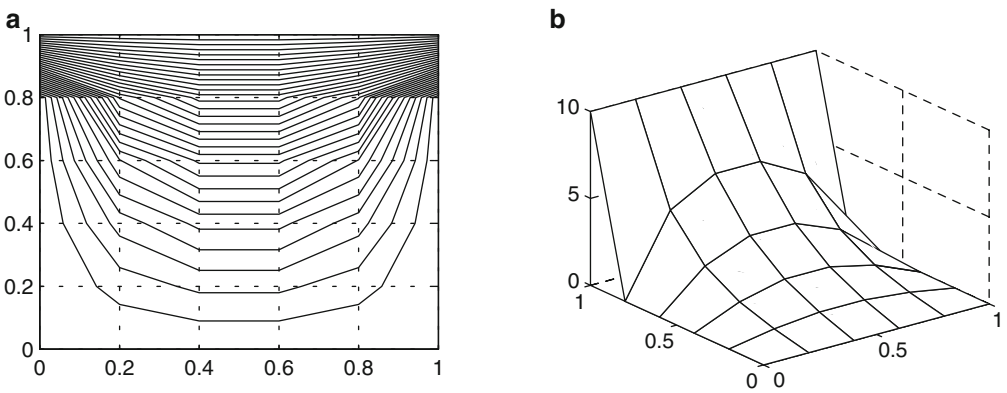

Figure 6.9 (**a**) Representation of results as a contour plot of constant potentials at increments of 0.3226 V. (**b**) Representation of the results as a three-dimensional plot. Height indicates potential

[1] The plots in **Figures 6.9a** and **6.9b** were drawn with Matlab, using the data in **Figure 6.8**.

6.3.3.2 Explicit Solution

In an explicit solution, we start with **Eq. (6.15)** and assume that all potentials are known, including at interior nodes, at any step of the solution. Steps 1, 2, 3, and 6 are identical to those for the implicit solution. The differences between the implicit and explicit methods are in Steps 4 and 5.

Step 4: Approximation Before applying the approximation in **Eq. (6.15)**, all interior potentials are set to zero for lack of a better choice. This is the guess required to start the solution. If we have any basis for a better guess, it should be used, but the initial guess is not terribly important. Any reasonable guess will lead to a correct solution.

Evaluation of the potential at node (i, j) consists of calculating the average of the four potentials above, below, to its left, and to its right as indicated in **Eq. (6.15)**. The only additional constraint is that any potential that is updated is then used for the evaluation of subsequent potentials.

As examples, the potentials at points 1, 2, 3, 4, 5, and 6 (in **Figure 6.7a**) are calculated as

$$V_1 = \frac{10+0+0+0}{4} = 2.5 \text{ V}, \qquad V_2 = \frac{2.5+10+0+0}{4} = 3.125 \text{ V}$$

$$V_3 = \frac{3.125+10+0+0}{4} = 3.28125 \text{ V}, \qquad V_4 = \frac{3.28125+10+0+0}{4} = 3.3203125 \text{ V}$$

$$V_5 = \frac{0+2.5+0+0}{4} = 0.625 \text{ V}, \qquad V_6 = \frac{0.625+3.125+0+0}{4} = 0.9375 \text{ V}$$

Note that in the approximation, the latest, most up-to-date value of the point is always used.

Step 5: Solution The solution proceeds similarly with all other nodes. At each step, a nodal value is calculated as an average of the previously known nodes. After 16 steps, one iteration through the mesh is completed and a new solution is obtained. This solution is shown in **Figure 6.10a**. Comparing this solution with that obtained for the implicit solution in **Figure 6.8** (which is exact within the round-off errors of computation) or with the analytic solution, this is obviously not the "correct" solution. Thus, we repeat the process, again starting with node 1, assuming that the value at node 1 is unknown and evaluating it in terms of the neighboring nodes using the solution in **Figure 6.10a** as the new guess. After repeating the solution three more times, we obtain the solution in **Figure 6.10b**. This solution is closer but still not "correct." To obtain an "accurate" solution, we repeat this process until the change in solution is lower than a predetermined tolerance value. To see how the solution progresses, consider **Figure 6.11**, which shows the solution at point 5 as a function of the iterations employed. After about 15 iterations, the solution is within 0.1 % of the exact solution, whereas after 20 iterations, it is within 0.01 % of the exact solution. The solution, therefore, converges to the exact solution (in this plot, $V_5 = 2.2348$ V) as the number of iterations increases, and provided the number of iterations is sufficiently large, an accurate solution will be obtained.

a

10.0	10.0	10.0	10.0	10.0	10.0
0.0	2.5	3.125	3.2813	3.3203	0.0
0.0	**0.625**	0.9375	1.0547	1.0938	0.0
0.0	0.1563	0.2734	0.3320	0.3564	0.0
0.0	0.0391	0.0781	0.1025	0.1147	0.0
0.0	0.0	0.0	0.0	0.0	0.0

b

10.0	10.0	10.0	10.0	10.0	10.0
0.0	4.1418	5.4189	5.5217	4.3353	0.0
0.0	**1.7464**	2.6459	2.7655	1.9699	0.0
0.0	0.7227	1.1993	1.2890	0.8892	0.0
0.0	0.2691	0.4702	0.5142	0.3508	0.0
0.0	0.0	0.0	0.0	0.0	0.0

Figure 6.10 Solution to geometry in **Figure 6.6**. (**a**) After one iteration. (**b**) After four iterations. Node 5 is emphasized for reference

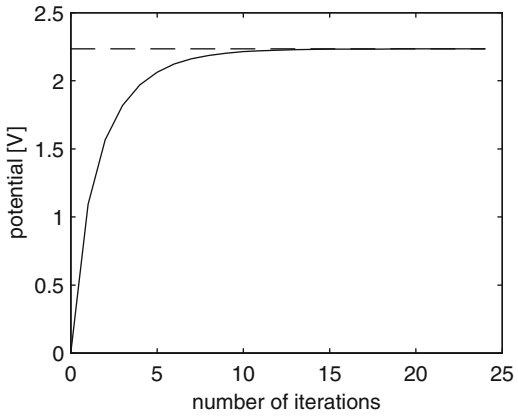

Figure 6.11 Solution at node 5 (**Figure 6.7a**) as a function of number of the iterations

The only remaining question is how to stop the iteration procedure so that an acceptable solution is obtained. We could obviously choose one node and follow the solution at this node. Since, in general, the correct solution is not known, all we can do is look at the change in solution, and when the change in the solution between subsequent iterations is lower than a given error, we view the solution is acceptable.

This can be written as

$$\left|V_i^n - V_i^{n-1}\right| \leq e \tag{6.19}$$

This is very simple but has the disadvantage that we infer the correctness of the solution throughout the solution domain based on a single node. If the solution also converges at all other nodes at the same rate (a fact we normally do not know and have no reason to assume), this approach is very good. More appropriate would be a measure of convergence that takes into account the changes at all nodes. A possible error criterion is an average error per node:

$$\frac{1}{N}\sum_{i=1}^{N}\left|V_i^n - V_i^{n-1}\right| \leq e \tag{6.20}$$

The process described here is an iterative process and is explicit in that the solution is known at each iteration of the process. Explicit procedures are preferred over implicit methods, particularly when very large grids are required and the implicit procedure would be prohibitively slow.

The results shown here were obtained with the program **fdmexp.m**. The results for the last (24th) iteration with an error tolerance $e = 10^{-4}$ are shown in **Figure 6.12**. Note that the results are very close to those from the implicit solution in **Figure 6.8**.

10.0	10.0	10.0	10.0	10.0	10.0
0.0	4.5454	5.9469	5.9469	4.5454	0.0
0.0	**2.2347**	3.2953	3.2953	2.2348	0.0
0.0	1.0984	1.7044	1.7045	1.0984	0.0
0.0	0.4545	0.7196	0.7197	0.4545	0.0
0.0	0.0	0.0	0.0	0.0	0.0

Figure 6.12 Two-dimensional finite difference results. Explicit solution for a 5×5 mesh with an error tolerance of 5×10^{-5}. The output for the last (24th) iteration is listed with node 5 emphasized

6.3.4 Solution to Poisson's Equation

So far, we discussed only the solution to Laplace's equation. The extension of the above results to Poisson's equation is rather simple. The difference is merely in the approximation which was given in **Eq. (6.17)**. In the implicit approach, we normally write the approximation as

$$4V_{i,j} - V_{i-1,j} - V_{i+1,j} - V_{i,j-1} - V_{i,j+1} = h^2 \frac{\rho_{i,j}}{\varepsilon_{i,j}} \tag{6.21}$$

In the explicit solution, the form in **Eq. (6.17)** is used directly:

$$V_{i,j} = \frac{V_{i-1,j} + V_{i+1,j} + V_{i,j-1} + V_{i,j+1}}{4} + \frac{h^2 \rho_{ij}}{4\varepsilon_{ij}} \tag{6.22}$$

Note, however, that these approximations are fundamentally different than those for Laplace's equation in that now the approximation depends on the distance between the nodes ($\Delta x = \Delta y = h$). We will have to take this into account and choose a small enough distance to provide an accurate solution. This may seem to be a difficult task because, after all, how do we know what value to choose? In practice, we will chose some value and solve the problem, and if we want to make sure the choice is good, we may choose a second, smaller value (such as half the previous value of h) and repeat the solution. If the solution does not change, or changes very little, the choice was acceptable. If not, we may repeat this process until we are satisfied with the choice. Note, also, that the extra term in Poisson's equation applies only at those nodes at which there is a charge density. At any other node, we use the approximation to Laplace's equation.

Exercise 6.2 Find the finite difference approximation for the three-dimensional Laplace's equation for implicit and explicit solutions.

Answer

$$6V_{i,j,k} - V_{i-1,j,k} - V_{i+1,j,k} - V_{i,j-1,k} - V_{i,j+1,k} - V_{i,j,k-1} - V_{i,j,k+1} = 0 \quad \text{(implicit)}$$
$$V_{i,j,k} = \frac{V_{i-1,j,k} - V_{i+1,j,k} - V_{i,j-1,k} - V_{i,j+1,k} - V_{i,j,k-1} - V_{i,j,k+1}}{6} \quad \text{(explicit)}$$

Exercise 6.3 Find the finite difference approximation for the three-dimensional Poisson's equation for implicit and explicit solutions.

Answer

$$6V_{i,j,k} - V_{i-1,j,k} - V_{i+1,j,k} - V_{i,j-1,k} - V_{i,j+1,k} - V_{i,j,k-1} - V_{i,j,k+1} = \frac{h^2 \rho_{i,j,k}}{\varepsilon_{i,j,k}} \quad \text{(implicit)}$$
$$V_{i,j,k} = \frac{V_{i-1,j,k} - V_{i+1,j,k} - V_{i,j-1,k} - V_{i,j+1,k} - V_{i,j,k-1} - V_{i,j,k+1}}{6} + \frac{h^2 \rho_{i,j,k}}{6\varepsilon_{i,j,k}} \quad \text{(explicit)}$$

Example 6.1 Solution to the One-Dimensional Poisson's Equation Consider a parallel plate capacitor as in **Figure 6.13a**. The capacitor is connected to a potential difference of 100 V, but, in addition, the dielectric between the plates contains a volume charge density which is a function of the distance between the plates given as $\rho_v = -2.5 \times 10^{-3}(x^2 - 0.1x)$ [C/m^3]. Assume the y and z dimensions of the capacitor are very large so that edge effects may be neglected and the material between the plates to be dielectric with relative permittivity of 4:

(a) Find the potential distribution everywhere between the two plates.
(b) Find the electric field intensity everywhere between the plates.

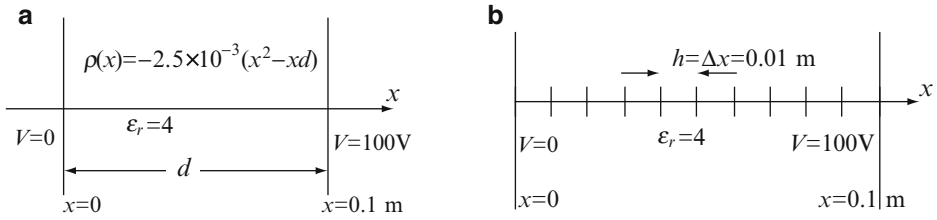

Figure 6.13 (**a**) Parallel plate capacitor with charge density between the plates connected to a potential difference. (**b**) Finite difference discretization

Solution:

(a) Because the potential only varies with the x dimension, the problem may be solved using the one-dimensional Poisson's equation. The capacitor is replaced with an equivalent geometry shown in **Figure 6.13b**. The distance between the plates is divided into $k = 10$ subdomains, resulting in nine unknown potential values in addition to the two known potentials on the boundaries. Although this problem has an analytic solution and the problem may, in fact, be solved by hand, we will use the computer program because, in general, hand calculation is too tedious.

The potential distribution in the capacitor as obtained using program **fdm1d.m** is shown in **Figure 6.14a**. The analytic solution for this problem was obtained in **Section 5.4.2** [**Eq. (5.11)**; see also **Example 5.1**].

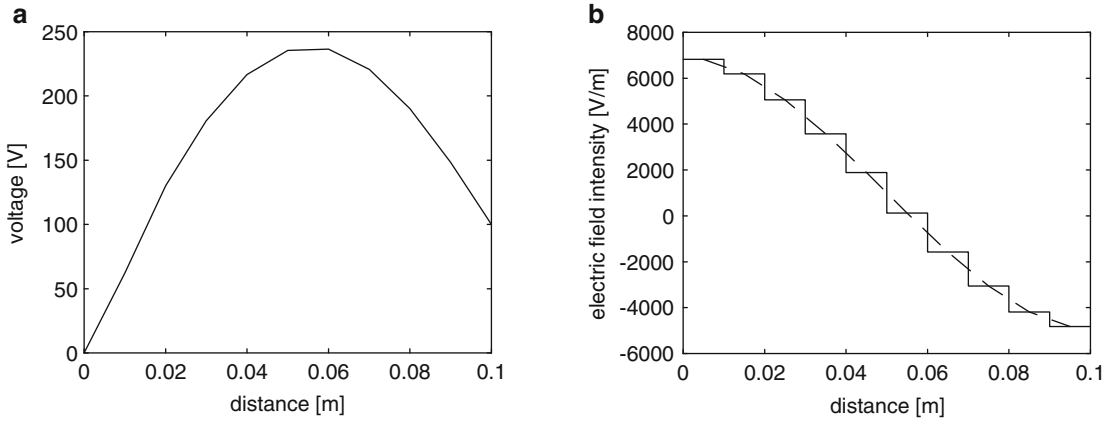

Figure 6.14 Solution for the problem in **Figure 6.13a**. (**a**) Solution for potential. (**b**) Solution for electric field intensity. Negative sign indicates the field is in the negative x direction

(b) The electric field intensity is calculated from the potentials at the various points using **Eqs. (6.1), (6.2),** or **(6.3)**. By definition, the electric field intensity is

$$\mathbf{E} = -\nabla V = -\hat{\mathbf{x}}\frac{dV(x)}{dx} \quad \left[\frac{\text{V}}{\text{m}}\right]$$

After the potential values at all points in the mesh are known, the electric field intensity is written using **Figure 6.13b** and **Eq. (6.2)** as

$$\mathbf{E}_i = -\hat{\mathbf{x}}\left(\frac{V_{i+1} - V_i}{\Delta x}\right) \quad \left[\frac{\text{V}}{\text{m}}\right]$$

This electric field intensity is calculated for each space between two potential values and is assumed to be constant between the potentials.

Program **fdm1d.m** solves both for the potential and electric field intensity. A plot of the electric field intensity is shown in **Figure 6.14b**. Note that it is a staircase plot because the gradient of the potential remains constant between each two potential points. The accuracy of these results may be easily improved by using a larger number of points.

Example 6.2 Two-Dimensional Poisson's Equation: Solution Using Irregular Boundaries Consider the geometry in **Figure 6.15a**. The upper plate is a half-cylinder and forms, together with the lower plate, a capacitor. The potential difference between the upper and lower plates is $V = 24$ V and the plates are separated a distance of 20 mm at the edges. Assume free space throughout:

(a) Calculate the potential distribution between the plates.
(b) A charge density of 10^{-6} C/m^3 is added, uniformly distributed between the plates. Calculate the potential distribution everywhere and compare with **(a)**.

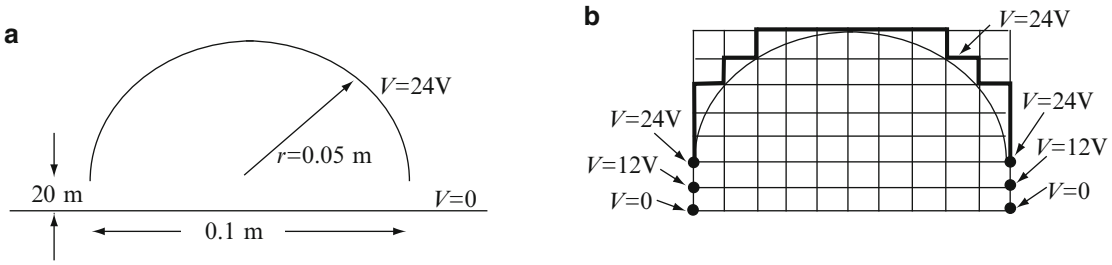

Figure 6.15 (**a**) Capacitor made of a cylindrical plate over a flat plate (shown in cross section). (**b**) Rectangular grid over the geometry in (**a**)

Solution: Although the geometry here is two-dimensional, the upper surface is curved and it would seem that a rectangular, uniform grid is not suitable for analysis of this problem. To analyze the problem, we first fit a uniform grid over the geometry as shown in **Figure 6.15b**. Then, we modify the surface of the upper plate such that it follows points on the grid by moving the surface to the nearest grid point, as shown in **Figure 6.15b** (thick line). This may seem as taking too much liberty with the geometry, and, in fact, for the grid shown, it is. However, in the limit, as we increase the number of points, the approximate and exact surfaces are close. To simplify analysis, we will assume that all points above the upper surface are at the potential of the upper surface. The latter assumption is equivalent to making the upper conductor fill the space above the surface up to the top boundary. This does not entail any approximation on the potential between the two surfaces.

Now, we have a uniform grid in which all points which are not between the two surfaces are boundary nodes. At the point where the two surfaces are closest to each other, we must also specify boundary conditions. Since we do not know the conditions at these locations, we simply assume that the potential varies linearly and specify the value at the nodes as half the potential difference between the plates as shown in **Figure 6.15b**.

The potential is found using program **fdm2d.m**, using the iterative method for Poisson's equation. In this case, it is most convenient to plot equal potential lines because the surface is curved. The plots in **Figure 6.16** were obtained using the grid in **Figure 6.15b**. Note that in **Figure 6.16b**, the potential between the plates can be higher than the boundary potentials because of the charge density that exists between the plates.

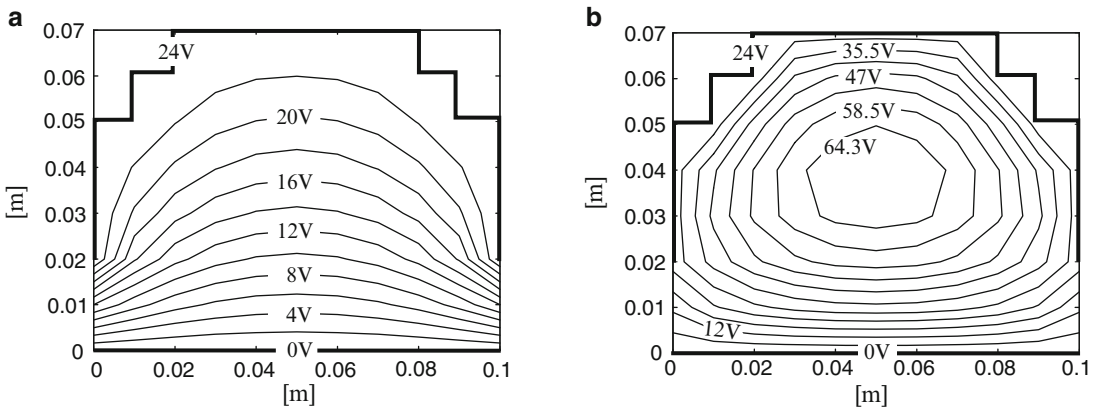

Figure 6.16 Solution for the capacitor in **Figure 6.15a** Equal potential lines are shown. (**a**) Potential distribution without space charge. (**b**) Distribution with charge density of 10^{-6} C/m^3 between the plates

Example 6.3 Three-Dimensional Laplace's Equation The three-dimensional box in **Figure 6.17a** is given. The upper plate is connected to a 10 V potential and the other five plates are grounded (0 V). Find the potential and electric field intensity everywhere inside the box.

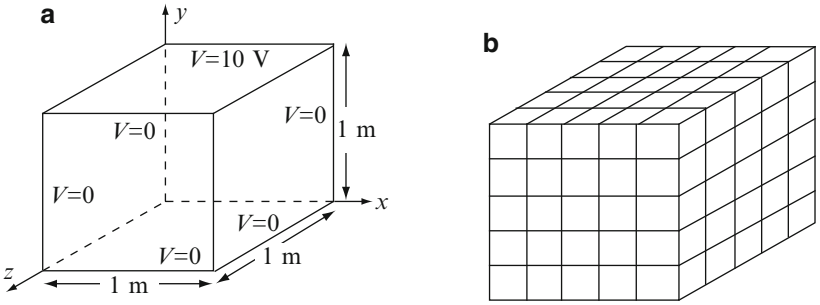

Figure 6.17 (**a**) Conducting box with given boundary potentials. (**b**) 5 × 5 × 5 finite difference grid over the box

Solution: The solution of three-dimensional problems is usually much more complicated than two-dimensional applications. However, the finite difference method uses a rectangular grid and the bookkeeping is not too difficult. The approximation here is that for Laplace's equation given in **Exercise 6.2**.

A three-dimensional grid, with five divisions in each direction, is defined over the mesh as shown in **Figure 6.17b**. The mesh has a total of 64 internal nodes which must be evaluated. The solution follows almost identical steps as for the two-dimensional solution in **Section 6.3.3**.

One difficulty encountered in three-dimensional applications is in the display of data. Usually, a few cross sections are cut and the potential drawn on these planes. Two contour plots are shown in **Figures 6.18a** and **6.18b**. The first is for a cross section cut vertically at $x = 0.6$, parallel to the y–z plane. The second is a horizontal cut through at $z = 0.6$, parallel to the x–y plane. Three-dimensional plots may also be drawn as shown in **Figure 6.19**. The latter is drawn for a 10 × 10 × 10 grid.

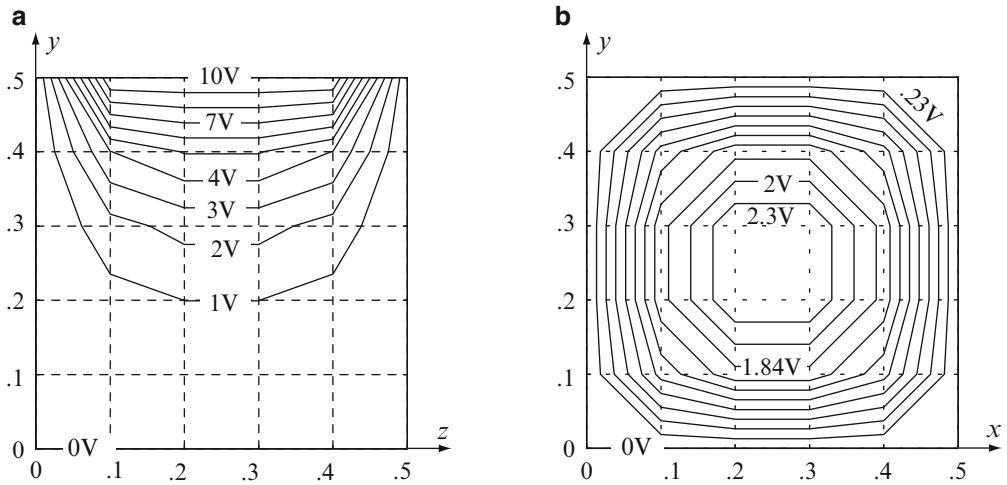

Figure 6.18 (**a**) Contour plot on a cross section cut vertically at $x = 0.6$. (**b**) Contour plot on a cross section cut horizontally at $z = 0.6$. Both plots are for the 5 × 5 × 5 grid

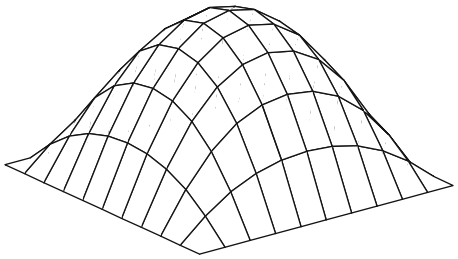

Figure 6.19 Three-dimensional plot of the potential distribution in the box ($10 \times 10 \times 10$ mesh, horizontal cut at $z = 0.5$ m)

To calculate the electric field intensity, we use the potential difference between every two neighboring nodes, as was done in **Example 6.1**. However, now there are three directions in space. Application of **Eq. (6.2)** in the x, y, and z directions provides the electric field intensities on the edges of the grid. The method is shown in **Figure 6.20** and a list of the electric field intensities at a few mesh locations is given in **Table 6.1**. Note that different components are evaluated at different locations on the grid. It is also possible to calculate the average of the electric fields in each direction and associate these averages with the center of the cell in **Figure 6.20**. These calculations were performed using program **fdm3d.m**.

Table 6.1 Electric field intensity at a few locations in the $10 \times 10 \times 10$ grid

x	y	z	E_x	E_y	E_z
0.3 m	0.2 m	0.2 m	0.4235 V/m	*	*
0.6 m	0.5 m	0.8 m	*	0.0 V/m	*
0.6 m	0.6 m	0.9 m	*	*	24.652 V/m
0.7 m	0.2 m	0.2 m	−0.4235 V/m	*	*
0.2 m	0.7 m	0.2 m	*	−0.4235 V/m	*
0.2 m	0.2 m	0.3 m	*	*	1.422 V/m

*Indicates that the corresponding component is not calculated at this location

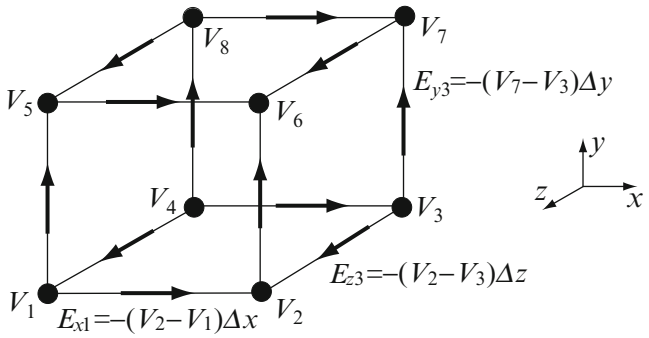

Figure 6.20 Calculation of electric fields from potentials, using **Eq. (6.2)**

6.4 The Method of Moments: An Intuitive Approach

Consider, again, the calculation of the electric potential from known charge density distributions. Suppose we know the charge distribution in a given section of the space Ω. Then, from **Eq. (4.33)**, the potential a distance R from the charge distribution is

$$V(x,y,z) = \int_{\Omega'} \frac{1}{4\pi\varepsilon R} \rho_{\Omega'}\left(x',y',z'\right) d\Omega' \quad [\text{V}] \tag{6.23}$$

where Ω' denotes the domain in which the charge distribution is known and primed coordinates are used to distinguish between the source and observation points (at which the potential is calculated). The domain Ω' can be a surface s', a length l', or a volume v'. In all cases, the formula for the calculation of the potential has exactly the same form. In even more general terms, the equation may be written as

$$V(x,y,z) = \int_{\Omega'} K\left(x,y,z,x',y',z'\right)\rho_{\Omega'}\left(x',y',z'\right)d\Omega' \quad [\text{V}] \tag{6.24}$$

where K is a geometric function (called the kernel of the integral) relating the measured quantity V and the source ρ. In this notation, the method can be applied to any integral of this form, whatever the measured quantity and source.

The question now is the following: Suppose the charge density ρ_s is not known but, instead, the potential is known. Can we also use this relation to calculate the charge density distribution? The answer is yes, but only under certain conditions. To see how this can be done in general, we use the example in **Figure 6.21a**. It consists of a very thin charged conducting surface layer with a general surface charge density $\rho_s(x',y',z')$ [C/m^2]. The charge density is not known, but the potential on the conducting surface is known and equal to V_0. The goal is to calculate the charge density everywhere on the surface.

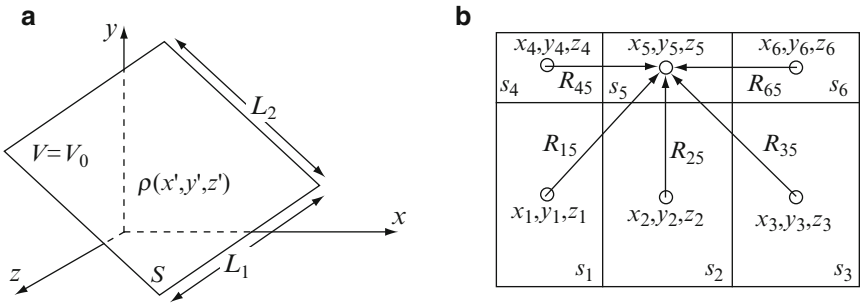

Figure 6.21 (**a**) A charged surface with known potential and unknown surface charge density distribution. (**b**) Division of the charged surface in (**a**) into six subdomains. The charge density in each subdomain is unknown but constant

The first hint at what we must do is from **Eq. (6.23)**. For the charge density to be calculable, it must be taken outside the integral sign. This, in turn, means that the charge density must be constant on the surface. This condition cannot be met in general; therefore, we resort to dividing the surface into a large number of subsurfaces and assume that for each subsurface, the charge density is constant, but it may vary from subsurface to subsurface. An example of the subdivision of the surface into subdomains is shown in **Figure 6.21b**, where six subdomains are used. The premise behind this approach is that since we are free to divide the surface into as many subdomains as we wish, we can make this approximation as good as needed by simply increasing the number of subdomains. In the limit, each subdomain is infinitesimally small and we are back to the expression in **Eq. (6.23)**. To formulate the method we divide the surface into N subdomains and assume a uniform charge density ρ_{si} [C/m^2] on subdomain s_i'. The potential at an arbitrary point (x_j,y_j,z_j) on subdomain j is

$$V\left(x_j,y_j,z_j\right) = \sum_{i=1}^{N}\int_{s_i'} \frac{\rho_{si}}{4\pi\varepsilon R_{ij}\left(x_i',y_i',z_i',x_j,y_j,z_j\right)}ds_i' = \sum_{i=1}^{N}\frac{\rho_{si}}{4\pi\varepsilon}\int_{s_i'}\frac{1}{R_{ij}\left(x_i',y_i',z_i',x_j,y_j,z_j\right)}ds_i' \quad [\text{V}] \tag{6.25}$$

where R_{ij} is the distance between the location of ds_i' and the point at which the potential is calculated. Next, we assume that the total charge on subdomain i, which is equal to $q_{si} = \rho_{si}s_i$, is located at the center of subdomain i. The potential on subdomain j is constant on the subdomain:

$$V_j = \frac{1}{4\pi\varepsilon}\sum_{\substack{i=1\\ i\neq j}}^{N}\frac{\rho_{si}s_i}{R_{ij}\left(x_i',y_i',z_i',x_j,y_j,z_j\right)} + V_{\rho_{sj}} \quad [\text{V}] \tag{6.26}$$

The distance R_{ij} is

$$R_{ij}\left(x_i',y_i',z_i',x_j,y_j,z_j\right) = \sqrt{\left(x_j-x_i'\right)^2+\left(y_j-y_i'\right)^2+\left(z_j-z_i'\right)^2} \tag{6.27}$$

The first term in **Eq. (6.26)** is the potential at the center of subdomain j, due to $N-1$ point charges located at the centers of all subdomains except subdomain j. The second term is the potential at the center of subdomain j due to the charge density

on subdomain j. This term must be calculated separately since if we use the formula for point charges we obtain an infinite potential ($R_{ij} = 0$).

The computation sequence for the potential at $j = 5$ is shown schematically in **Figure 6.21b**. The relationship between subdomains i and j ($i \neq j$) is shown in **Figure 6.22a**.

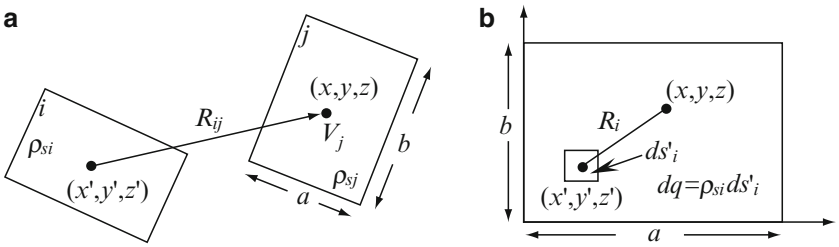

Figure 6.22 (**a**) Relation between potential on subdomain j and charge density on subdomain i. (**b**) Calculation of the potential at the center of subdomain i due to its own charge

A number of points must be indicated here:

(1) The expression in the integral in **Eq. (6.25)** is a purely geometrical expression. It only has to do with the surface of subdomain i and the distance between this subdomain and the point at which the potential is calculated.
(2) There are N unknown values of ρ, one on each subdomain.
(3) To be able to evaluate N unknown values of the surface charge density, we must calculate the potential at N distinct points at which the potential is known. This provides N equations for the N unknown charge densities.

To use this method for practical calculation, we must define a systematic way of dividing the surface into subdomains and of calculating the potential V_j at N points. These decisions are made as follows:

(1) The surface is divided into N subdomains. The subdomains do not need to be equal in size but equal-sized subdomains simplify the solution and allow simple computer implementation.
(2) The number of subdomains can be as large as we wish. The larger the number of subdomains, the more accurate the solution, but also the lengthier the computation.
(3) The potential is calculated at the center of each of the subdomains and set to the known value at that point.

In effect, we have replaced the charged surface by equivalent point charges, each equal to $\rho_i s_i$, and placed these point charges at the center of the corresponding subdomain. It is now a simple matter of calculating the potentials and setting these to the known values at the centers of the subdomains. The general expressions for the potentials are

$$V_j = V_{\rho_{sj}} + \sum_{i=1,\, i\neq j}^{N} \rho_{si} \frac{s_i}{4\pi\varepsilon R_{ij}} \quad [\mathrm{V}], \qquad j = 1, 2, \ldots, N \tag{6.28}$$

To obtain a form amenable to computation, we rewrite **Eq. (6.28)** as

$$V_j = K_{jj}\rho_j + \sum_{\substack{i=1 \\ i\neq j}}^{N} \rho_i K_{ij} \quad [\mathrm{V}], \qquad j = 1, 2, \ldots, N \tag{6.29}$$

where the geometric function[2] is

$$K_{ij} = \frac{s_i}{4\pi\varepsilon\sqrt{\left(x_j - x_i'\right)^2 + \left(y_j - y_i'\right)^2 + \left(z_j - z_i'\right)^2}}, \qquad i, j = 1, 2, \ldots, N, \quad i \neq j \tag{6.30}$$

Note that the terms for which $i = j$ cannot be calculated using this expression because if we place a charge at a point, the potential at that point is infinite. The potential at point j due to the charge density on the subsurface j is calculated by direct

[2] The kernel K_{ij} is called here a "geometric" function. In fact, it is the potential at point j due to a unit point charge at point i. This function is also called the Green's function for the geometry. The resulting Green's function method of solution for Poisson's equation is an important method of solution for both analytic and numerical methods because once the solution for a unit source is obtained, the solution for any source is relatively easy to obtain. However, we will call the kernel a geometric function for simplicity because we do not pursue the idea of a Green's function in any detail.

integration. To do so, we assume a flat surface, of dimensions a and b, and with charge density $\rho(s) =$ constant as in **Figure 6.22b**. The potential at the center of the plate [point $(x_i,y_i,z_i) = (x_j,y_j,z_j)$] is found by direct integration (see **Exercise 6.4**) as

$$V(x_i, y_i, z_i) = \frac{\rho_{si}}{4\pi\varepsilon}\left(2a_i \ln\frac{b_i + \sqrt{a_i^2 + b_i^2}}{a_i} + 2b_i \ln\frac{a_i + \sqrt{a_i^2 + b_i^2}}{b_i}\right) \quad [\text{V}] \tag{6.31}$$

Therefore, the geometric function for $i = j$ is

$$K_{jj} = \frac{1}{4\pi\varepsilon}\left(2a_j \ln\frac{b_j + \sqrt{a_j^2 + b_j^2}}{a_j} + 2b_j \ln\frac{a_j + \sqrt{a_j^2 + b_j^2}}{b_j}\right) \tag{6.32}$$

With this, we can use **Eq. (6.29)** for all values of i, j.

The computation sequence starts by dividing the surface in **Figure 6.21a** into N equal subdomains ($N = 6$ in this case), as shown in **Figure 6.21b**. For convenience, we will assume equal-sized rectangles with constant charge density on each rectangle. The centers of the subdomains are points (x_j,y_j,z_j). Using **Eq. (6.29)**, in expanded form, the potential at each of the six points is

$$\begin{gathered}
\rho_{s1}K_{1,1} + \rho_{s2}K_{1,2} + \rho_{s3}K_{1,3} + \cdots + \rho_{sN-1}K_{1,N-1} + \rho_{sN}K_{1,N} = V_1 \\
\rho_{s1}K_{2,1} + \rho_{s2}K_{2,2} + \rho_{s3}K_{2,3} + \cdots + \rho_{sN-1}K_{2,N-1} + \rho_{sN}K_{2,N} = V_2 \\
\vdots \\
\rho_{s1}K_{N-1,1} + \rho_{s2}K_{N-1,2} + \rho_{s3}K_{N-1,3} + \cdots + \rho_{sN-1}K_{N-1,N-1} + \rho_{sN}K_{N-1,N} = V_{N-1} \\
\rho_{s1}K_{N,1} + \rho_{s2}K_{N,2} + \rho_{s3}K_{N,3} + \cdots + \rho_{sN-1}K_{N,N-1} + \rho_{sN}K_{N,N} = V_N
\end{gathered} \tag{6.33}$$

Rewriting this as a matrix system, we get

$$\begin{bmatrix}
K_{1,1} & K_{1,2} & K_{1,3} & \cdots & K_{1,N-1} & K_{1,N} \\
K_{2,1} & K_{2,2} & K_{2,3} & \cdots & K_{2,N-1} & K_{2,N} \\
\vdots & \vdots & \vdots & \vdots & \vdots & \vdots \\
K_{N-1,1} & K_{N-1,2} & K_{N-1,3} & \cdots & K_{N-1,N-1} & K_{N-1,N} \\
K_{N,1} & K_{N,2} & K_{N,3} & \cdots & K_{N,N-1} & K_{N,N}
\end{bmatrix}
\begin{bmatrix}
\rho_{s1} \\ \rho_{s2} \\ \vdots \\ \rho_{sN-1} \\ \rho_{sN}
\end{bmatrix}
=
\begin{bmatrix}
V_1 \\ V_2 \\ \vdots \\ V_{N-1} \\ V_N
\end{bmatrix} \tag{6.34}$$

Note that $K_{ij} = K_{ji}$; that is, the system of equations is symmetric.

This system can be solved in any convenient manner. For a small system, hand calculation or the use of a programmable calculator may be sufficient. For larger systems, a computer will almost always have to be used. Once the charge density has been calculated everywhere on the conducting surface, it may be used in many ways. For example, we may want to calculate the capacitance of the plate or the electric field intensity anywhere in space. Some of the possible uses of the method are shown in the examples that follow. The method is rather general and applies to other types of fields as well. Also, we may use the same method to calculate the charge density on surfaces, inside volumes, or on thin or thick lines. The only fundamental requirement of the method is to find a simple relation between charge and potential in this case, or between the source and the fields in the general case.

Exercise 6.4 Derive **Eq. (6.31)** for a rectangular surface, charged with a constant surface charge density ρ_s [C/m^2]. Assume dimensions of the plate are a [m] and b [m], define a differential area $ds = dx'dy'$, and calculate the potential at the center of the plate by direct integration over the surface of the plate. Use **Figure 6.22b**, assume the plate is in the $x-y$ plane and the general point (x,y) is at (0,0).

Example 6.4 Application: Charge and Capacitance of an Electrode The flat electrode in **Figure 6.23a** is given:

(a) If the potential on the plate is 1 V, what is the total charge on the plate?
(b) Find the capacitance of the plate.
(c) Find the electric field intensity at a height of 2 m above the center of the plate.

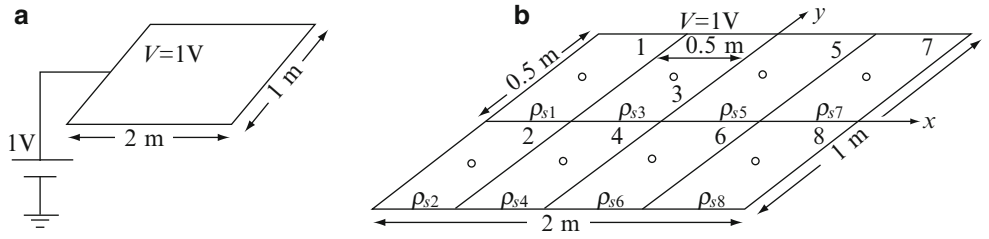

Figure 6.23 (**a**) Charged rectangular electrode held at a constant potential of 1 V. (**b**) Division of the electrode into eight equal subdomains, each with constant unknown charge density

Solution: For convenience, we place the plate on the x–y plane with the center at the origin and divide the plate into eight equal subsurfaces as shown in **Figure 6.23b**. This subdivision may not be sufficient to obtain an accurate solution, but, for now, this discretization is used so that we may give the actual matrix entries. Also, with a matrix of this size, hand calculation is possible. The computer program **mom1.m** is used to obtain more accurate solutions:

(a) To calculate the unknown charge densities, the locations of the centers of the subdomains are first identified. With the sides of the plate parallel to the axes, the centers of the subdomains are P_1 (−0.75,0.25), P_2 (−0.75,−0.25), P_3 (−0.25, 0.25), P_4 (−0.25,−0.25), P_5 (0.25,0.25), P_6 (0.25,−0.25), P_7 (0.75,0.25), and P_8 (0.75,−0.25). The permittivity of free space is 8.854×10^{-12} F/m and the size of each subdomain is $a_i = 0.5$ m and $b_i = 0.5$ m, and, therefore, $s_i = 0.25$ m^2. The plate is at 1 V potential with respect to infinity. With these, we can now go back to **Eq. (6.30)** and calculate K_{ij} and to **Eq. (6.32)** to calculate K_{jj}. The resulting matrix is

$$10^{10} \times \begin{bmatrix} 1.59 & .450 & .450 & .318 & .225 & .201 & .150 & .142 \\ .450 & 1.59 & .318 & .450 & .201 & .225 & .142 & .150 \\ .450 & .318 & 1.59 & .450 & .450 & .318 & .225 & .201 \\ .318 & .450 & .450 & 1.59 & .318 & .450 & .201 & .225 \\ .225 & .201 & .450 & .318 & 1.59 & .450 & .450 & .318 \\ .201 & .225 & .318 & .450 & .450 & 1.59 & .318 & .450 \\ .150 & .142 & .225 & .201 & .450 & .318 & 1.59 & .450 \\ .142 & .150 & .201 & .225 & .318 & .450 & .450 & 1.59 \end{bmatrix} \begin{bmatrix} \rho_{s1} \\ \rho_{s2} \\ \rho_{s3} \\ \rho_{s4} \\ \rho_{s5} \\ \rho_{s6} \\ \rho_{s7} \\ \rho_{s8} \end{bmatrix} = \begin{bmatrix} 1 \\ 1 \\ 1 \\ 1 \\ 1 \\ 1 \\ 1 \\ 1 \end{bmatrix}$$

Using the program **mom1.m** or solving the matrix using a programmable calculator gives the charge densities as follows:

$$\rho_{s1} = \rho_{s2} = \rho_{s7} = \rho_{s8} = 0.31572 \times 10^{-10} \quad [\text{C/m}^2]$$

and

$$\rho_{s3} = \rho_{s4} = \rho_{s5} = \rho_{s6} = 0.22241 \times 10^{-10} \quad [\text{C/m}^2]$$

The total charge on the plate is the sum of the charges of the individual domains:

$$Q = \sum_{i=1}^{8} \rho_{si} s_i = 4 \times 0.25 \times 0.31572 \times 10^{-10} + 4 \times 0.25 \times 0.22241 \times 10^{-10}$$
$$= 0.538 \times 10^{-10} \quad [\text{C}].$$

(b) To find the capacitance of the plate, we divide the total charge by the potential difference between the plate and the reference point at infinity:

$$C = \frac{Q}{V} = \frac{0.538 \times 10^{-10}}{1} = 53.8 \quad [\text{pF}]$$

Because we only used eight subdomains to describe a 2 m^2 plate, we should expect some error. To check the relative error, the number of subdomains is increased and the capacitance calculated using the program **mom1.m**. The results are as follows:

Number of subdomains	4 × 2	8 × 4	16 × 8	20 × 10	24 × 12
Capacitance	53.8 pF	56.5 pF	57.9 pF	58.2 pF	58.4 pF

The result can be improved as much as we wish by increasing the number of subdomains. Unfortunately, this has its limits: The computer can be easily overwhelmed if we get carried away with the number of subdomains. Note that for a division of 24 × 12, the program solves a 288 × 288 system of equations with a full matrix. If we were to increase the division to, say, 50 × 50, a 2,500 × 2,500 system must be solved.

(c) To calculate the electric field intensity at the center and above the plate, we note that the subdomains are symmetric about the center of the plate. This means that each two symmetric charges cancel each other's horizontal component of the electric field intensity. Using **Figure 6.24**, the electric field intensity at point *P* may be written as follows:

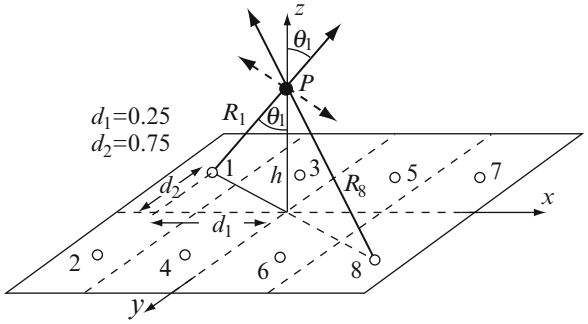

Figure 6.24 Calculation of the electric field intensity above the center of the plate in **Figure 6.23a**

Due to point 1: The total charge at point (1) is $Q_1 = 0.25 \times 0.31572 \times 10^{-10} = 7.893 \times 10^{-12}$ C. The vertical component of the electric field intensity due to point (1) is

$$E_1 = \frac{Q_1}{4\pi\varepsilon_0 R_1^2}\cos\theta_1 = \frac{Q_1 h}{4\pi\varepsilon_0 R_1^2 R_1} = \frac{Q_1 h}{4\pi\varepsilon_0\left(d_1^2 + d_2^2 + h^2\right)^{3/2}}$$
$$= \frac{7.893 \times 10^{-12} \times 2}{4 \times \pi \times 8.854 \times 10^{-12} \times \left(0.25^2 + 0.75^2 + 2^2\right)^{3/2}} = 0.0143 \quad \left[\frac{\text{V}}{\text{m}}\right]$$

Each of the four corner subdomains (1), (2), (7), and (8) produces identical fields. Similarly, due to point (5), the total charge at point (5) is $Q_5 = 0.25 \times 0.22241 \times 10^{-10} = 5.56 \times 10^{-12}$ C. The electric field intensity at point *P* due to this charge is

$$E_5 = \frac{Q_5}{4\pi\varepsilon_0 R_5^2}\cos\theta_5 = \frac{5.56 \times 10^{-12} \times 2}{4 \times \pi \times 8.854 \times 10^{-12} \times \left(0.25^2 + 0.25^2 + 2^2\right)^{3/2}} = 0.0119 \quad \left[\frac{\text{V}}{\text{m}}\right]$$

The fields due to points (3), (4), (5), and (6) are identical. Thus, the total field is in the positive *z* direction (positive charges) and equal to

$$\mathbf{E}_{total} = \hat{\mathbf{z}}\,4(0.0119 + 0.0143) = \hat{\mathbf{z}}\,0.105 \quad [\text{V/m}]$$

Program **mom1.m** solves for the charge and capacitance for a rectangular plate of any dimensions and with any number of subdomains. The program may be easily adapted for other applications.

Example 6.5 Capacitance Between Two Conducting Strips The two strips in **Figure 6.25a** represent two general conductors. The strips are 50 mm wide and 1 m long and are separated a distance of 100 mm vertically. Calculate the capacitance between the two strips if:

(a) The two strips are parallel to each other ($\theta = 0°$).
(b) The strips are perpendicular to each other ($\theta = 90°$).

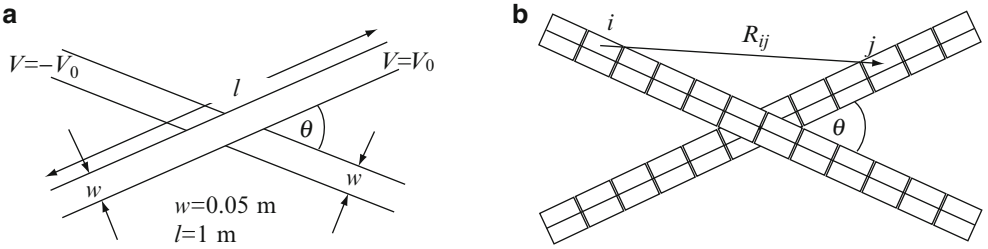

Figure 6.25 (**a**) Two conducting strips separated a distance d (vertically) and intersecting at an angle θ. (**b**) Division of the two strips into 24 subdomains each

Solution: Although the two strips form a parallel plate capacitor, the capacitance cannot be calculated using the parallel plate capacitor formula because of the very complicated electric fields which exist throughout space. Instead, we use the method of moments. To calculate capacitance, we assume a potential +1 V on the top plate and −1 V on the lower plate. The magnitude of the potential is immaterial but it must have a numerical value. The potential difference between the two conductors is 2 V.

Each plate is divided into an arbitrary number of subdomains which, in general, can be of arbitrary size. The division is shown schematically in **Figure 6.25b**, where each strip is shown subdivided into 24 equal subdomains. The number of domains that should be used depends on the accuracy required. Applying the division and using the dimensions in **Figure 6.25a**, with a total of 24 subdomains on each strip, the capacitance between the two strips is found to be 12.2 pF, using program **mom1.m**. This discretization is rather coarse. The capacitance for a number of discretization levels is shown in **Table 6.2**.

Table 6.2 Capacitance for parallel and crossed strips at various discretization levels

Discretization (each strip)	6 × 1	12 × 2	18 × 3
Capacitance*	12.59 pF	12.62 pF	12.74 pF
Capacitance†	9.75 pF	9.78 pF	10.1 pF

*Strips parallel to each other. †Strips perpendicular to each other

Example 6.6 Application: Inter-gate Capacitances in CMOS Devices In a CMOS (complementary metal oxide semiconductor) integrated circuit, the gates of two FETs (field effect transistors) are deposited on the surface of a silicon chip as shown in **Figure 6.26a**. One gate is 10 × 10 μm in size, the second is 20 × 20 μm, and the two are separated by 2 μm. The capacitance between the gates is important because it defines coupling between the gates; that is, when one gate is charged, the other acquires a charge too, because of the capacitance between them. If this capacitance is large, the second gate may be activated when it should not be. It is required to find the capacitance between the two gates. Assume the two plates are in free space and calculate the capacitance between the plates. In reality, one side of the plates is on silicon, which has a relative permittivity of about 12, but, for simplicity, we will assume the plates to be in free space.

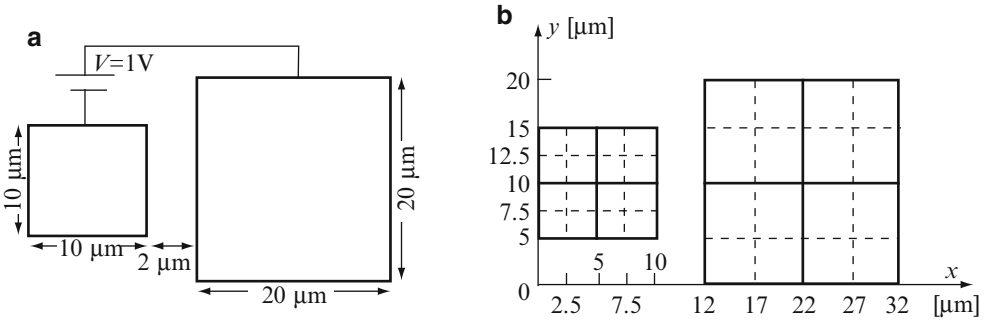

Figure 6.26 (**a**) A model for the gates of two field-effect transistors. (**b**) Coordinates and dimensions for evaluation of capacitance between the two gates in (**a**)

Solution: The solution here is similar to that in **Example 6.5**, but now we have two unequal plates. Therefore, we divide each plate into a number of subdomains and assume a potential difference of $V_0 = 1$ V between the two plates. Since the plates are unequal in size, it is not possible to assume that the plates are at equal and opposite potentials. Therefore, we assume one plate to be at potential V_A and the second at V_B, where $V_A + V_B = 1$ V. This leaves us with one unknown potential. The necessary additional relation comes from the fact that the total charge on the smaller plate and the total charge on the larger plate are equal in magnitude; that is, the potential must be such as to produce equal and opposite total charges on the two plates.

Next, we need to divide the plates into subdomains. We use different numbers of divisions but, on each plate, the subdomains are kept equal in size. To simplify the evaluation, we use the system of coordinates shown in **Figure 6.26b**. Each plate is divided into four equal subdomains for illustration purposes (solid lines). Other divisions may be used (see **Table 6.3**). The location of the centers is evaluated from the coordinates given and number of domains on each plate. Now, we again employ **Eqs. (6.30)** and **(6.32)** to evaluate the terms K_{ij} and K_{jj} for $i = 1$ to 8 and $j = 1$ to 8 (for the discretization shown in **Figure 6.26b**). The resulting matrix is 8 by 8 in size. To solve for the charge densities of the subdomains, we must first know the potential on each plate. Because the two plates are unequal in size, we do not know the exact values of the potentials on the plates that guarantee equal charge distribution on the plates. The actual potentials required for the charges on two plates to be equal in magnitude are computed iteratively: We assume an initial zero potential on one plate and 1 V on the second. In each iteration, the potential on both plates is reduced and the charges are evaluated and checked to see if the charges on the two plates are equal in magnitude. If they are, the solution is complete. If not, the iteration process is continued. The results for a number of discretizations are shown in **Table 6.3**.
Note: In **Table 6.3**, the first discretization in the first row is for the smaller plate, the second for the larger plate.

Table 6.3 Capacitance for different discretization levels

Discretization	$2 \times 2, 2 \times 2$	$2 \times 2, 4 \times 4$	$2 \times 2, 8 \times 8$	$4 \times 4, 4 \times 4$	$4 \times 4, 8 \times 8$
Capacitance [F]	0.3276×10^{-15}	0.3446×10^{-15}	0.3541×10^{-15}	0.3710×10^{-15}	0.3829×10^{-15}

Example 6.7 Method of Moments: Hand Computation In general, the system of equations produced by the method of moments is difficult to solve by hand and, if it is large, almost impossible. However, for a relatively small number of subdomains, hand computation is possible, especially if symmetry conditions are used to reduce computation. To show how hand computation may be used, **Example 6.6** is used here again, but, first, we look into the calculation of capacitance of a single plate.

Solution:

(a) Capacitance of the small plate.
Consider the smaller plate in **Figure 6.26a**. To calculate its capacitance, we divide the plate into 16 equal subdomains as shown in **Figure 6.27a**. At first glance, it would seem that we must solve a 16×16 system of equations. This is not the

case. Inspection of the geometry shows that the four corner subdomains must have equal charge and, therefore, equal charge densities because of symmetry. Similarly, subdomains 2, 3, 5, 9, 8, 12, 14, and 15 have the same charge densities. Subdomains 6, 7, 10, and 11 also have the same charge density. Thus, in effect, there are only three distinct charge densities that need to be calculated and only three equations in three unknowns need to be assembled and solved.

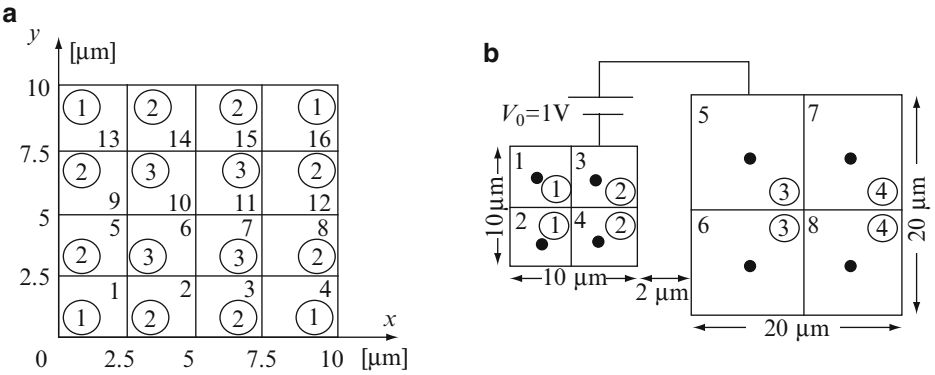

Figure 6.27 (**a**) Division of the smaller plate in **Figure 6.26a** into 16 subdomains. (**b**) Division of the geometry in **Figure 6.26a** for hand computation. Circled numbers indicate equal charge density

The solution proceeds by writing three distinct equations: one for subdomain 1, one for subdomain 2, and the third for subdomain 6. The three equations are

$$V_1 = \frac{1}{4\pi\varepsilon_0}\left\{\rho_1\left[K_{11}^{'} + \frac{2s}{R_{14}} + \frac{s}{R_{1,16}}\right] + \rho_2 s\left[\frac{2}{R_{12}} + \frac{2}{R_{13}} + \frac{2}{R_{18}} + \frac{2}{R_{1,12}}\right] + \rho_3 s\left[\frac{1}{R_{16}} + \frac{2}{R_{17}} + \frac{1}{R_{1,11}}\right]\right\} \quad [\text{V}]$$

$$V_2 = \frac{1}{4\pi\varepsilon_0}\left\{\rho_1 s\left[\frac{1}{R_{12}} + \frac{1}{R_{2,13}} + \frac{1}{R_{24}} + \frac{1}{R_{2,16}}\right] + \rho_2\left[K_{22}^{'} + \frac{s}{R_{23}} + \frac{s}{R_{25}} + \frac{2s}{R_{28}} + \frac{s}{R_{2,12}} + \frac{s}{R_{2,14}} + \frac{s}{R_{2,15}}\right]\right.$$
$$\left. + \rho_3 s\left[\frac{1}{R_{26}} + \frac{1}{R_{27}} + \frac{1}{R_{2,10}} + \frac{1}{R_{2,11}}\right]\right\} \quad [\text{V}]$$

$$V_6 = \frac{1}{4\pi\varepsilon_0}\left\{\rho_1 s\left[\frac{1}{R_{16}} + \frac{2}{R_{46}} + \frac{1}{R_{6,16}}\right] + \rho_2 s\left[\frac{2}{R_{26}} + \frac{2}{R_{36}} + \frac{2}{R_{68}} + \frac{2}{R_{6,12}}\right] + \rho_3\left[K_{66}^{'} + \frac{2s}{R_{67}} + \frac{s}{R_{6,11}}\right]\right\} \quad [\text{V}]$$

where the term $K_{jj}^{'}$ is the term in brackets in **Eq. (6.32)**. The various constants are as follows:

$$V_1 = V_2 = V_6 = 1 \quad [\text{V}]$$
$$a = 2.5 \times 10^{-6} \text{ m}, \quad b = 2.5 \times 10^{-6} \text{ m}$$
$$s = 2.5 \times 10^{-6} \times 2.5 \times 10^{-6} = 6.25 \times 10^{-12} \text{ m}^2$$
$$R_{12} = R_{23} = R_{26} = R_{67} = 2.5 \times 10^{-6} \text{ m}$$
$$R_{13} = R_{24} = R_{2,10} = R_{68} = 5.0 \times 10^{-6} \text{ m}$$
$$R_{14} = R_{2,14} = 7.5 \times 10^{-6} \text{ m}$$
$$R_{1,16} = 7.5\sqrt{2} \times 10^{-6} \text{ m}$$
$$R_{18} = R_{2,13} = R_{2,15} = \sqrt{(7.5)^2 + (2.5)^2} \times 10^{-6} = \sqrt{62.5} \times 10^{-6} \text{ m}$$
$$R_{1,12} = R_{2,16} = \sqrt{(7.5)^2 + (5)^2} \times 10^{-6} = \sqrt{81.25} \times 10^{-6} \text{ m}$$
$$R_{17} = R_{28} = R_{2,11} = R_{46} = R_{6,12} = \sqrt{(5)^2 + (2.5)^2} \times 10^{-6}$$
$$= \sqrt{31.25} \times 10^{-6} \text{ m}$$
$$R_{1,11} = R_{6,16} = R_{2,12} = 5\sqrt{2} \times 10^{-6} \text{ m}$$
$$R_{25} = R_{47} = R_{27} = R_{6,11} = R_{16} = R_{36} = 2.5\sqrt{2} \times 10^{-6} \text{ m}$$
$$K_{11}^{'} = K_{22}^{'} = K_{66}^{'} = 10 \times 10^{-6} \ln\left(1 + \sqrt{2}\right)$$

Denoting ρ_1 as the charge density on any of the corner subdomains (1, 4, 13, and 16); ρ_2 the charge density on any of subdomains 2, 3, 5, 9, 8, 12, 14, or 15; and ρ_3 the charge density on any of subdomains 6, 7, 10, or 11, and substituting the values above in the three equations above gives

$$1 = \frac{1}{4 \times \pi \times 8.854 \times 10^{-6}} \left\{ \rho_1 \left[10 \ \ln\left(1+\sqrt{2}\right) + \frac{12.5}{7.5} + \frac{6.25}{7.5\sqrt{2}} \right] + 6.25 \times \rho_2 \left[\frac{2}{2.5} + \frac{2}{5} + \frac{2}{\sqrt{62.5}} + \frac{2}{\sqrt{81.25}} \right] + 6.25 \times \rho_3 \left[\frac{1}{2.5\sqrt{2}} + \frac{2}{\sqrt{31.25}} + \frac{1}{5\sqrt{2}} \right] \right\} \quad [\text{V}]$$

$$1 = \frac{1}{4 \times \pi \times 8.854 \times 10^{-6}} \left\{ 6.25 \times \rho_1 \left[\frac{1}{2.5} + \frac{1}{\sqrt{62.5}} + \frac{1}{5} + \frac{1}{\sqrt{81.25}} \right] + \rho_2 \left[10 \ \ln\left(1+\sqrt{2}\right) + \frac{6.25}{2.5} + \frac{6.25}{2.5\sqrt{2}} + \frac{12.5}{\sqrt{31.25}} + \frac{6.25}{5\sqrt{2}} + \frac{6.25}{7.5} + \frac{6.25}{\sqrt{62.5}} \right] + 6.25 \times \rho_3 \left[\frac{1}{2.5} + \frac{1}{2.5\sqrt{2}} + \frac{1}{5} + \frac{1}{\sqrt{31.25}} \right] \right\} \quad [\text{V}]$$

$$1 = \frac{1}{4 \times \pi \times 8.854 \times 10^{-6}} \left\{ 6.25 \times \rho_1 \left[\frac{1}{2.5\sqrt{2}} + \frac{1}{\sqrt{31.25}} + \frac{1}{5\sqrt{2}} \right] + 6.25 \times \rho_2 \left[\frac{2}{2.5} + \frac{2}{2.5\sqrt{2}} + \frac{2}{5.0} + \frac{2}{\sqrt{31.25}} \right] + \rho_3 \left[10 \ \ln\left(1+\sqrt{2}\right) + \frac{12.5}{2.5} + \frac{6.25}{2.5\sqrt{2}} \right] \right\} \quad [\text{V}]$$

Simplifying these expressions gives

$$\begin{aligned} 1 &= 9.949 \times 10^4 \rho_1 + 9.408 \times 10^4 \rho_2 + 4.393 \times 10^4 \rho_3 \quad [\text{V}] \\ 1 &= 4.704 \times 10^4 \rho_1 + 1.602 \times 10^5 \rho_2 + 5.964 \times 10^4 \rho_3 \quad [\text{V}] \\ 1 &= 4.390 \times 10^4 \rho_1 + 1.193 \times 10^5 \rho_2 + 1.400 \times 10^5 \rho_3 \quad [\text{V}] \end{aligned}$$

Solution of this system of equations gives

$$\begin{aligned} \rho_1 &= 5.4755 \times 10^{-6} \ \text{C/m}^2, \\ \rho_2 &= 3.8295 \times 10^{-6} \ \text{C/m}^2, \\ \rho_3 &= 2.1613 \times 10^{-6} \ \text{C/m}^2 \end{aligned}$$

To calculate the capacitance of the plate, we first calculate the total charge. The latter is

$$Q = 4 \times 6.25 \times 10^{-12} \times 5.4755 \times 10^{-6} + 8 \times 6.25 \times 10^{-12} \times 3.8295 \times 10^{-6} + 4 \times 6.25 \times 10^{-12} \times 2.1613 \times 10^{-6} = 3.824 \times 10^{-16} \quad [\text{C}]$$

The capacitance is

$$C = \frac{Q}{V} = \frac{3.824 \times 10^{-16}}{1} = 3.824 \times 10^{-16} \quad [\text{F}].$$

(b) Capacitance between plates.

As a second example of hand computation, consider, again, **Figure 6.26a**. We wish to calculate the capacitance between the two plates. Because of symmetry about a horizontal line passing through the center of the geometry (see **Figure 6.27b**), there are only four different charge densities as shown. The equations for the four distinct charge densities (written for subdomains 1, 3, 5, and 7) are

$$V_1 = \frac{\rho_1}{4\pi\varepsilon_0}\left[K'_{11} + \frac{s_1}{R_{12}}\right] + \frac{\rho_2 s_1}{4\pi\varepsilon_0}\left[\frac{1}{R_{13}} + \frac{1}{R_{14}}\right] + \frac{\rho_3 s_2}{4\pi\varepsilon_0}\left[\frac{1}{R_{15}} + \frac{1}{R_{16}}\right] + \frac{\rho_4 s_2}{4\pi\varepsilon_0}\left[\frac{1}{R_{17}} + \frac{1}{R_{18}}\right] \quad [\text{V}]$$

$$V_1 = \frac{\rho_1 s_1}{4\pi\varepsilon_0}\left[\frac{1}{R_{13}} + \frac{1}{R_{23}}\right] + \frac{\rho_2}{4\pi\varepsilon_0}\left[K'_{33} + \frac{s_1}{R_{34}}\right] + \frac{\rho_3 s_2}{4\pi\varepsilon_0}\left[\frac{1}{R_{35}} + \frac{1}{R_{36}}\right] + \frac{\rho_4 s_2}{4\pi\varepsilon_0}\left[\frac{1}{R_{37}} + \frac{1}{R_{38}}\right] \quad [\text{V}]$$

$$V_2 = \frac{\rho_1 s_1}{4\pi\varepsilon_0}\left[\frac{1}{R_{15}} + \frac{1}{R_{25}}\right] + \frac{\rho_2 s_1}{4\pi\varepsilon_0}\left[\frac{1}{R_{35}} + \frac{1}{R_{45}}\right] + \frac{\rho_3}{4\pi\varepsilon_0}\left[K'_{55} + \frac{s_2}{R_{56}}\right] + \frac{\rho_4 s_2}{4\pi\varepsilon_0}\left[\frac{1}{R_{57}} + \frac{1}{R_{58}}\right] \quad [\text{V}]$$

$$V_2 = \frac{\rho_1 s_1}{4\pi\varepsilon_0}\left[\frac{1}{R_{17}} + \frac{1}{R_{27}}\right] + \frac{\rho_2 s_1}{4\pi\varepsilon_0}\left[\frac{1}{R_{37}} + \frac{1}{R_{47}}\right] + \frac{\rho_3 s_2}{4\pi\varepsilon_0}\left[\frac{1}{R_{57}} + \frac{1}{R_{67}}\right] + \frac{\rho_4}{4\pi\varepsilon_0}\left[K'_{77} + \frac{s_2}{R_{78}}\right] \quad [\text{V}]$$

In these, K'_{jj} are defined as in the previous example and the following are used:

$a = b = 5 \times 10^{-6}$ m
$s_1 = 5 \times 10^{-6} \times 5 \times 10^{-6} = 25 \times 10^{-12}$ m^2 on the small plate
$a = b = 10 \times 10^{-6}$ m
$s_2 = 10 \times 10^{-6} \times 10 \times 10^{-6} = 100 \times 10^{-12}$ m^2 on the large plate

$$R_{12} = R_{13} = R_{34} = 5 \times 10^{-6} \text{ m}, \quad R_{14} = R_{23} = 5\sqrt{2} \times 10^{-6} \text{ m}$$
$$R_{15} = \sqrt{(17-2.5)^2 + (5-2.5)^2} \times 10^{-6} = \sqrt{216.5} \times 10^{-6} \text{ m}$$
$$R_{16} = R_{25} = \sqrt{(17-2.5)^2 + (-5-2.5)^2} \times 10^{-6} = \sqrt{266.5} \times 10^{-6} \text{ m}$$
$$R_{17} = \sqrt{(27-2.5)^2 + (5-2.5)^2} \times 10^{-6} = \sqrt{606.5} \times 10^{-6} \text{ m}$$
$$R_{18} = R_{27} = \sqrt{(27-2.5)^2 + (-5-2.5)^2} \times 10^{-6} = \sqrt{656.5} \times 10^{-6} \text{ m}$$
$$R_{35} = \sqrt{(17-7.5)^2 + (2.5-5)^2} \times 10^{-6} = \sqrt{96.5} \times 10^{-6} \text{ m}$$
$$R_{36} = R_{45} = \sqrt{(17-7.5)^2 + (2.5+5)^2} \times 10^{-6} = \sqrt{146.5} \times 10^{-6} \text{ m}$$
$$R_{37} = \sqrt{(27-7.5)^2 + (5-2.5)^2} \times 10^{-6} = \sqrt{386.5} \times 10^{-6} \text{ m}$$
$$R_{38} = R_{47} = \sqrt{(27-7.5)^2 + (-5-2.5)^2} \times 10^{-6} = \sqrt{436.5} \times 10^{-6} \text{ m}$$
$$R_{56} = \mathrm{R}_{57} = R_{78} = 10 \times 10^{-6} \text{ m}, \quad R_{58} = R_{67} = 10\sqrt{2} \times 10^{-6} \text{ m}$$

In this case, $K_{11} = K_{33}$ and $K_{55} = K_{77}$. From **Eq. (6.32)**, we get

$$K'_{11} = K'_{33} = 20 \times 10^{-6} \ \ln\left(1+\sqrt{2}\right), \quad K'_{55} = K'_{77} = 40 \times 10^{-6} \ \ln\left(1+\sqrt{2}\right)$$

Substituting these values into the four equations, we get

$$V_1 = \frac{1}{4 \times \pi \times 8.854 \times 10^{-6}}\left\{\rho_1\left[20\ln\left(1+\sqrt{2}\right) + \frac{25}{5}\right] + 25 \times \rho_2\left[\frac{1}{5} + \frac{1}{5\sqrt{2}}\right] + 100 \times \rho_3\left[\frac{1}{\sqrt{216.5}} + \frac{1}{\sqrt{266.5}}\right] + 100 \times \rho_4\left[\frac{1}{\sqrt{606.5}} + \frac{1}{\sqrt{656.5}}\right]\right\} \quad [\text{V}]$$

$$V_1 = \frac{1}{4 \times \pi \times 8.854 \times 10^{-6}}\left\{25 \times \rho_1\left[\frac{1}{5} + \frac{1}{5\sqrt{2}}\right] + \rho_2\left[20 \ \ln\left(1+\sqrt{2}\right) + \frac{25}{5}\right] + 100 \times \rho_3\left[\frac{1}{\sqrt{96.5}} + \frac{1}{\sqrt{146.5}}\right] + 100 \times \rho_4\left[\frac{1}{\sqrt{386.5}} + \frac{1}{\sqrt{436.5}}\right]\right\} \quad [\text{V}]$$

$$V_2 = \frac{1}{4 \times \pi \times 8.854 \times 10^{-6}} \left\{ 100 \times \rho_1 \left[\frac{1}{\sqrt{216.5}} + \frac{1}{\sqrt{266.5}} \right] + 25 \times \rho_2 \left[\frac{1}{\sqrt{96.5}} + \frac{1}{\sqrt{146.5}} \right] + \rho_3 \left[40 \ \ln\left(1 + \sqrt{2}\right) + \frac{100}{10} \right] + 100 \times \rho_4 \left[\frac{1}{10} + \frac{1}{10\sqrt{2}} \right] \right\} \quad [\text{V}]$$

$$V_2 = \frac{1}{4 \times \pi \times 8.854 \times 10^{-6}} \left\{ 100 \times \rho_1 \left[\frac{1}{\sqrt{606.5}} + \frac{1}{\sqrt{656.5}} \right] + 25 \times \rho_2 \left[\frac{1}{\sqrt{386.5}} + \frac{1}{\sqrt{436.5}} \right] + 100 \times \rho_3 \left[\frac{1}{10} + \frac{1}{10\sqrt{2}} \right] + \rho_4 \left[40 \ \ln\left(1 + \sqrt{2}\right) + \frac{100}{10} \right] \right\} \quad [\text{V}]$$

Since the potentials V_1 and V_2 are not known but the potential difference is known, we write

$$V_1 - V_2 = V_0 = 1.0 \ \text{V} \qquad \rightarrow \qquad V_1 = 1.0 + V_2 \quad [\text{V}]$$

The fifth equation necessary is the equality of charge on the two plates:

$$2\rho_1 s_1 + 2\rho_2 s_2 = -(2\rho_3 s_3 + 2\rho_4 s_4)$$

The negative sign on the right-hand side indicates the fact that the charge on plate (2) must be negative if the charge on plate (1) is positive. Thus, we assume potential V_2 to be an unknown to be determined and write the following five equations:

$$\begin{aligned}
1.0 + V_2 &= 2.034 \times 10^5 \rho_1 + 7.672 \times 10^4 \rho_2 + 1.161 \times 10^5 \rho_3 + 7.157 \times 10^4 \rho_4 \\
1.0 + V_2 &= 7.672 \times 10^4 \rho_1 + 2.034 \times 10^5 \rho_2 + 1.658 \times 10^5 \rho_3 + 8.874 \times 10^4 \rho_4 \\
V_2 &= 2.904 \times 10^4 \rho_1 + 4.148 \times 10^4 \rho_2 + 4.067 \times 10^5 \rho_3 + 1.534 \times 10^5 \rho_4 \\
V_2 &= 1.789 \times 10^4 \rho_1 + 2.218 \times 10^4 \rho_2 + 1.534 \times 10^5 \rho_3 + 4.067 \times 10^5 \rho_4 \\
50\rho_1 + 50\rho_2 + 200\rho_3 + 200\rho_4 &= 0
\end{aligned}$$

Solution of these five equations in five unknowns gives the charge densities ρ_1, ρ_2, ρ_3, and ρ_4 and the potential V_2:

$$\begin{aligned}
\rho_1 &= 3.0345 \times 10^{-6} \ \text{C/m}^2 \\
\rho_2 &= 3.5176 \times 10^{-6} \ \text{C/m}^2 \\
\rho_3 &= -1.0194 \times 10^{-6} \ \text{C/m}^2 \\
\rho_4 &= -6.1860 \times 10^{-7} \ \text{C/m}^2 \\
V_2 &= -0.27569 \ \text{V}.
\end{aligned}$$

Note that the potential V_2 does not equal V_1 in magnitude ($V_1 = 1.0 + V_2 = 0.72431$ V) as required. To calculate the capacitance, we calculate the total charge density on either plate. On the small plate

$$Q_1 = 2 \times 3.0345 \times 10^{-6} \times 25 \times 10^{-12} + 2 \times 3.5176 \times 10^{-6} \times 25 \times 10^{-12} = 3.276 \times 10^{-16} \ \text{C}$$

On the larger plate

$$Q_2 = -2 \times 1.0194 \times 10^{-6} \times 100 \times 10^{-12} - 2 \times 6.1860 \times 10^{-7} \times 100 \times 10^{-12} = -3.276 \times 10^{-16} \ \text{C}$$

The two charges are equal in magnitude (within the computation error) and opposite in sign as required. Taking the charge on the smaller (or larger) plate and dividing by the potential difference between the plates gives the capacitance:

$$C = \frac{Q}{V} = \frac{3.276 \times 10^{-16}}{1} = 3.276 \times 10^{-16} \ \text{F}$$

Note that the capacitance calculated here is virtually identical to that calculated in **Example 6.6** (first column in **Table 6.3**).

Exercise 6.5 Find the equations required for hand calculation of the charge densities in **Example 6.4**, using the subdomains in **Figure 6.23b**. Find the capacitance and compare to that found in **Example 6.4**.

Answer

$$\frac{\rho_1}{4\pi\varepsilon_0}\left[K'_{11}+\frac{s_2}{R_{12}}+\frac{s_7}{R_{17}}+\frac{s_8}{R_{18}}\right]+\frac{\rho_3}{4\pi\varepsilon_0}\left[\frac{s_3}{R_{13}}+\frac{s_4}{R_{14}}+\frac{s_5}{R_{15}}+\frac{s_6}{R_{16}}\right]=1$$

$$\frac{\rho_1}{4\pi\varepsilon_0}\left[\frac{s_1}{R_{13}}+\frac{s_2}{R_{23}}+\frac{s_7}{R_{37}}+\frac{s_8}{R_{38}}\right]+\frac{\rho_3}{4\pi\varepsilon_0}\left[K'_{33}+\frac{s_4}{R_{34}}+\frac{s_5}{R_{35}}+\frac{s_6}{R_{36}}\right]=1$$

where

$$s_1=s_2=s_3=s_4=s_5=s_6=s_7=s_8=0.25\ \text{m}^2$$

$$K'_{11}=K'_{33}=1.76275$$

$$\rho_1=\rho_2=\rho_7=\rho_8,\qquad \rho_3=\rho_4=\rho_5=\rho_6$$

$$R_{12}=R_{13}=R_{34}=R_{35}=0.5\ \text{m},\qquad R_{14}=R_{23}=R_{36}=0.5\sqrt{2}\ \text{m},$$

$$R_{37}=R_{15}=1\ \text{m},\qquad R_{38}=R_{16}=\sqrt{1.25}\ \text{m},$$

$$R_{17}=1.5\ \text{m},\qquad R_{18}=\sqrt{2.5}\ \text{m}$$

$C=53.81$ pF, virtually the same as in **Example 6.4** (first column).

6.5 The Finite Element Method: Introduction

The finite element method is rather new; it dates only to the early 1950s, but it has evolved into a highly sophisticated and useful method for the solution of a very large number of engineering problems, in all disciplines. The method is different than both the finite difference method and the method of moments. It consists of the division of the solution domain into subdomains, called ***finite elements***, in the form of spatial subdomains of finite length, area, or volume, as shown in **Figure 6.28** (for surface elements). Each element is defined by a number of edges, which define its space. The intersection of every two edges defines a ***node***. The assemblage of elements forms a ***mesh*** which must follow certain rules. The first and foremost of these is that elements must be of finite size. Second, the elements must be compatible. The latter property is explained in **Figures 6.29a** and **6.29b**.

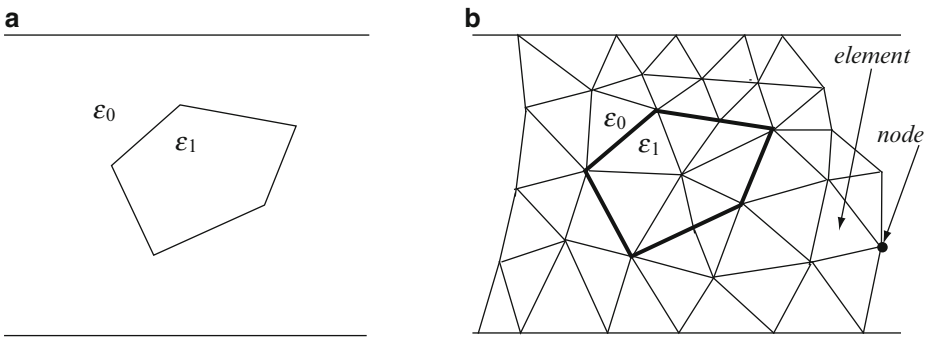

Figure 6.28 (**a**) A simple geometry with two materials to be discretized into finite elements. (**b**) A finite element discretization (partial) of the geometry in (**a**) using triangular finite elements

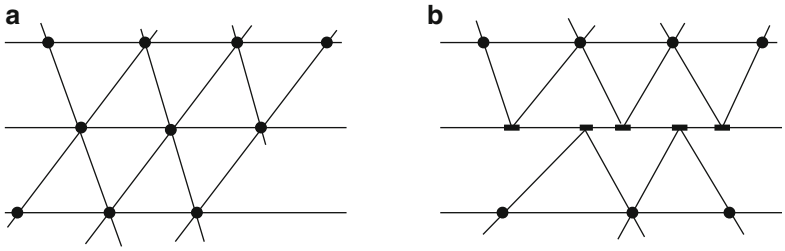

Figure 6.29 (**a**) A compatible mesh. Only triangle vertices form nodes. (**b**) A noncompatible mesh. Some of the nodes are located along edges

Finite elements can be of different sizes such that in regions where we anticipate larger variations in fields, the number of elements and their sizes can be changed to obtain higher element densities. In regions of lower fields, the number of elements can be lower. Each element can contain a different material; therefore, the interface between two different materials must coincide with element boundaries, as shown in **Figure 6.28b**.

The finite element method is somewhat more involved than the finite difference method and the method of moments, both in terms of the approximation it uses and in geometrical aspects of setting up the problem. Like the method of moments, it always results in a system of equations which must be solved.

We introduce the method by first discussing the concept of a finite element and the approximation involved, followed by the implementation of the finite element method for Poisson's equation. Then, we define the general procedure for solution and apply this to a number of examples.

6.5.1 The Finite Element

Definition of a finite element is the first step in any finite element analysis. There are many ways by which a finite element may be defined as there are different types of elements and methods of analysis. We will restrict ourselves, however, to one element, in two dimensions: the triangular element. The element should be viewed as a volume with unit depth. Therefore, whenever we discuss the area of the element, a volume is in fact implied. The finite element chosen also defines the approximation we can use. The only possible approximation on a simple triangle is a linear approximation in both spatial variables.

6.5.1.1 The Triangular Element

The triangle in **Figure 6.30** has three nodes and a finite area. The approximation within the element is assumed to be linear and of the form

$$V(x,y) = \alpha_1 + \alpha_2 x + \alpha_3 y \quad [\text{V}] \tag{6.35}$$

where the coefficients α_1, α_2, and α_3 remain to be determined and $V(x,y)$ is the solution defined within the finite element, including its nodes and edges. In this discussion, the solution is the electric potential, but it may be any other function. To determine the coefficients, we use **Figure 6.30** and write for the three nodes of the element:

$$V_i = \alpha_1 + \alpha_2 x_i + \alpha_3 y_i \quad [\text{V}] \tag{6.36}$$

$$V_j = \alpha_1 + \alpha_2 x_j + \alpha_3 y_j \quad [\text{V}] \tag{6.37}$$

$$V_k = \alpha_1 + \alpha_2 x_k + \alpha_3 y_k \quad [\text{V}] \tag{6.38}$$

Solving these three equations for the three unknowns α_1, α_2, and α_3 gives

$$\alpha_1 = \frac{1}{2\Delta}\left[\left(x_j y_k - x_k y_j\right)V_i + (x_k y_i - x_i y_k)V_j + \left(x_i y_j - x_j y_i\right)V_k\right] \tag{6.39}$$

$$\alpha_2 = \frac{1}{2\Delta}\left[\left(y_j - y_k\right)V_i + (y_k - y_i)V_j + \left(y_i - y_j\right)V_k\right] \tag{6.40}$$

$$\alpha_3 = \frac{1}{2\Delta}\left[\left(x_k - x_j\right)V_i + \left(x_i - x_k\right)V_j + \left(x_j - x_i\right)V_k\right] \tag{6.41}$$

where Δ is the area of the triangle and is given by

$$2\Delta = \begin{vmatrix} 1 & x_i & y_i \\ 1 & x_j & y_j \\ 1 & x_k & y_k \end{vmatrix} = \left(x_j y_k - x_k y_j\right) + \left(x_k y_i - x_i y_k\right) + \left(x_i y_j - x_j y_i\right) \tag{6.42}$$

These are now substituted into the approximation in **Eq. (6.35)** to obtain

$$\boxed{V(x,y) = N_i V_i + N_j V_j + N_k V_k \qquad [\text{V}]} \tag{6.43}$$

where the functions N_i, N_j, and N_k are

$$N_i = \frac{1}{2\Delta}\left[\left(x_j y_k - x_k y_j\right) + \left(y_j - y_k\right)x + \left(x_k - x_j\right)y\right] \tag{6.44}$$

$$N_j = \frac{1}{2\Delta}\left[\left(x_k y_i - x_i y_k\right) + \left(y_k - y_i\right)x + \left(x_i - x_k\right)y\right] \tag{6.45}$$

$$N_k = \frac{1}{2\Delta}\left[\left(x_i y_j - x_j y_i\right) + \left(y_i - y_j\right)x + \left(x_j - x_i\right)y\right] \tag{6.46}$$

These three functions are called the ***shape functions*** for the element because they only depend on the dimensions or "shape" of the element and have nothing to do with the unknown function $V\,(x,y)$. The shape functions have the following properties:

(1) $N_i = 1$ at node i and $N_i = 0$ at all other nodes, $N_j = 1$ at node j and $N_j = 0$ at all other nodes, and $N_k = 1$ at node k and $N_k = 0$ at all other nodes.

(2) The sum of the shape functions is equal to 1 at any point within the element and on its boundaries:

$$N_i + N_j + N_k = \sum_{l=i,j,k} N_l = 1 \tag{6.47}$$

This property can be verified directly from **Eqs. (6.44)** through **(6.46)** for any triangle (see **Exercise 6.6**). The above properties are general and hold for any finite element, regardless of shape, dimensionality, and method of defining the finite element.

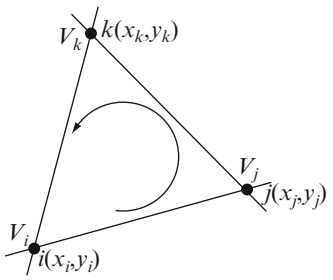

Figure 6.30 The three nodes of a general triangular element. Nodes must be ordered in a counterclockwise sequence

The derivatives of the shape functions with respect to x and y are evaluated directly from **Eqs. (6.44)** through **(6.46)**:

$$\frac{\partial N_i}{\partial x} = \frac{1}{2\Delta}\left(y_j - y_k\right), \qquad \frac{\partial N_i}{\partial y} = \frac{1}{2\Delta}\left(x_k - x_j\right) \tag{6.48}$$

$$\frac{\partial N_j}{\partial x} = \frac{1}{2\Delta}(y_k - y_i), \qquad \frac{\partial N_j}{\partial y} = \frac{1}{2\Delta}(x_i - x_k) \tag{6.49}$$

$$\frac{\partial N_k}{\partial x} = \frac{1}{2\Delta}\big(y_i - y_j\big), \qquad \frac{\partial N_k}{\partial y} = \frac{1}{2\Delta}\big(x_j - x_i\big) \tag{6.50}$$

These provide the approximation to the derivatives of the potential as

$$\boxed{\frac{\partial V(x,y)}{\partial x} = \frac{\partial N_i}{\partial x}V_i + \frac{\partial N_j}{\partial x}V_j + \frac{\partial N_k}{\partial x}V_k} \tag{6.51}$$

$$\boxed{\frac{\partial V(x,y)}{\partial y} = \frac{\partial N_i}{\partial y}V_i + \frac{\partial N_j}{\partial y}V_j + \frac{\partial N_k}{\partial y}V_k} \tag{6.52}$$

Equation (6.43) is the approximation of the function everywhere in the finite element and **Eqs. (6.51)** and **(6.52)** are its derivatives. These are at the heart of the finite element method. Before proceeding, we wish to write the shape functions, their derivatives, and the approximations for potential and their derivatives in a more compact form to avoid tedious operations later. We therefore denote the following:

$$p_i = x_j y_k - x_k y_j, \qquad p_j = x_k y_i - x_i y_k, \qquad p_k = x_i y_j - x_j y_i \tag{6.53}$$

$$q_i = y_j - y_k, \qquad q_j = y_k - y_i, \qquad q_k = y_i - y_j \tag{6.54}$$

$$r_i = x_k - x_j, \qquad r_j = x_i - x_k, \qquad r_k = x_j - x_i \tag{6.55}$$

The shape functions and their derivatives may be written as

$$N_l = \frac{1}{2\Delta}(p_l + q_l x + r_l y) \quad \text{and} \quad \frac{\partial N_l}{\partial x} = \frac{q_l}{2\Delta}, \quad \frac{\partial N_l}{\partial y} = \frac{r_l}{2\Delta}, \quad l = i, j, k \tag{6.56}$$

With these, the approximations for the potential and its derivatives are

$$\boxed{V(x,y) = \sum_{l=i,j,k} \frac{1}{2\Delta}(p_l + q_l x + r_l y)V_l = \sum_{l=i,j,k} N_l V_l \quad [\text{V}]} \tag{6.57}$$

$$\boxed{\frac{\partial V(x,y)}{\partial x} = \sum_{l=i,j,k} \frac{q_l}{2\Delta}V_l, \quad \frac{\partial V(x,y)}{\partial y} = \sum_{l=i,j,k} \frac{r_l}{2\Delta}V_l} \tag{6.58}$$

We will use these in the next section to define the finite element solution process.

After the potential is evaluated everywhere (as shown in the following sections), the electric field intensity may be evaluated from the potential, thus providing a complete solution to any electrostatic problem. The electric field intensity is found from the relation $\mathbf{E} = -\nabla V$ as

$$\mathbf{E} = \hat{\mathbf{x}}E_x + \hat{\mathbf{y}}E_y = -\hat{\mathbf{x}}\frac{\partial V}{\partial x} - \hat{\mathbf{y}}\frac{\partial V}{\partial y} \quad \left[\frac{\text{V}}{\text{m}}\right] \tag{6.59}$$

Using **Eq. (6.58)**, we get

$$E_x = -\sum_{l=i,j,k} \frac{q_l}{2\Delta}V_l \quad \text{and} \quad E_y = -\sum_{l=i,j,k} \frac{r_l}{2\Delta}V_l \quad \left[\frac{\text{V}}{\text{m}}\right] \tag{6.60}$$

These components are independent of x and y; they are constant in an element, as can be expected since the potential varies linearly within the element. Now, the nature of the approximation is even more apparent. The analytic solution is normally continuous and the electric field varies smoothly in the solution domain (except at interfaces between different materials). On the other hand, the numerical solution is discontinuous.

Exercise 6.6

(a) Show that $N_i = 1$ at node $i(x_i,y_i)$ and zero at nodes $j(x_j,y_j)$ and $k(x_k,y_k)$ by setting $x = x_i$ and $y = y_i$, then setting $x = x_j$ and $y = y_j$, and then setting $x = x_k$ and $y = y_k$ in **Eq. (6.43)**.

(b) Show that the sum of the shape functions anywhere within the finite element equals 1 by summing **Eqs. (6.44)** through **(6.46)**.

6.5.2 Implementation of the Finite Element Method

6.5.2.1 The Field Equations

So far, we obtained a general approximation for the potential in a finite element. The approximation should satisfy Poisson's and Laplace's equations simply because of the uniqueness theorem. A quick inspection reveals that if we were to substitute the approximation in **Eq. (6.57)** into Laplace's or Poisson's equations, the left-hand side is identically zero since the approximation is first-order in x and y, whereas the equations require second-order derivatives. There are two approaches we can take to extricate ourselves from this difficulty. One, and the most obvious, is to use higher-order approximations in x and y. The second is to modify the equations we solve so that only first-order derivatives are required. Surprisingly perhaps, we take the second route but with a twist: We look for a new function, which contains first-order derivatives only and whose solution provides a correct solution to the original equation (Laplace's or Poisson's equation in this case). To put these ideas in very simple and concrete terms, suppose we need to solve the equation $ax + b = 0$. We could solve it directly, but, we could also proceed in the following fashion:

(a) Find a function which, when minimized, provides a solution to the original equation. An appropriate function is

$$f(x) = \frac{ax^2}{2} + bx + c. \tag{6.61}$$

(b) Find the minimum of this function. Assuming that this function has a minimum, it corresponds to the point where $df/dx = 0$:

$$\frac{df(x)}{dx} = ax + b = 0 \tag{6.62}$$

which is the equation we wish to solve.

You may question this process: it is certainly more complicated in the case given here. More important is the question: How do we come up with the appropriate function and how do we guarantee that its minimum does provide the correct solution to the original problem? The answer to the first question is that there are systematic methods to obtain the appropriate function. As for the second, we can prove mathematically that the function provides the correct solution. However, we will do neither. Instead, we will rely on the time-honored method of "guessing" the function, finding the solution, and then verifying that it is a correct solution. Fortunately, this need only be done once since the function then applies to all electrostatic problems. In electrostatic applications as well as others, an appropriate function is the potential energy in the solution domain. The method consists of minimization of an energy function instead of solving directly the physical equation (in this case $\nabla^2 V = 0$ or $\nabla^2 V = -\rho/\varepsilon$). For a given domain, extending over a volume v, the energy function is

$$F(E) = \int_v \left[\frac{\varepsilon}{2}E^2 - \rho V\right] dv \tag{6.63}$$

where the first part is the energy stored in the electric field and the second is the energy in the sources that may exist in the solution domain. However, our problem is in two dimensions. Thus, we assume the solution domain to be made of a volume

of unit depth in the third dimension (for example, z) and of area s in the plane. In this case, the element of volume is $dv = 1ds$ and the integration is on the surface of the solution domain:

$$F(E) = \int_s \left[\frac{\varepsilon}{2}E^2 - \rho V\right] ds \tag{6.64}$$

Now that we have established the energy in the system, we use this as the function to minimize. First, we must rewrite **Eq. (6.64)** in terms of the potential rather than the electric field intensity. In Laplace's equation, there are no sources ($\rho = 0$) and the only potential energy is due to the electric field intensity in the solution domain. Because $E^2 = \mathbf{E} \cdot \mathbf{E}$, the energy function is [see **Eq. (6.59)**]

$$F(V) = \int_s \frac{\varepsilon}{2}\left[\left(\frac{\partial V}{\partial x}\right)^2 + \left(\frac{\partial V}{\partial y}\right)^2\right] ds \tag{6.65}$$

If, on the other hand, there are also sources in the solution domain, the appropriate energy function for Poisson's equation is

$$F(V) = \int_s \left[\frac{\varepsilon}{2}\left\{\left(\frac{\partial V}{\partial x}\right)^2 + \left(\frac{\partial V}{\partial y}\right)^2\right\} - \rho V\right] ds \tag{6.66}$$

From here on, we will discuss only Poisson's equation and the energy function associated with it. Laplace's equation, its energy function, and all other aspects of finite element implementation are obtained by simply setting the volume charge density ρ to zero. Note that **Eqs. (6.65)** and **(6.66)** contain only first-order derivatives as required, and the first-order approximation for the potential can be used.

6.5.2.2 Discretization

The second step in a finite element implementation is discretization of the solution domain into any number of finite elements that may be required to properly model the physical domain. After the physical domain is properly defined, the interior of the domain is divided into elements. This simply means that the coordinates of all nodes in the solution domain are defined and the appropriate nodes are associated with each element. Thus, for each element in the solution domain, we obtain:

(1) Coordinates of the three nodes of element N : $x_i, y_i, x_j, y_j, x_k, y_k$.
(2) Node numbers associated with element N : i, j, k.
(3) The material properties of all elements. In this case, this means associating with each element a value for permittivity.
(4) On those elements that have charge density, the charge density must be identified with the element.

These steps constitute the definition of a finite element mesh. In addition, we must identify those nodes that happen to be on the boundary of the mesh and the potential values prescribed on these nodes.

6.5.2.3 Minimization

In the minimization process, we perform the following:

(1) The energy function is evaluated for each element in turn.
(2) The derivative of the energy function with respect to each unknown in the element is calculated and set to zero.

The idea of discretization is to form the solution domain by an assemblage of finite elements. The energy function for the solution domain is then the sum of the energy functions of individual finite elements:

$$F(V) = \sum_{m=1}^{M} F_m \tag{6.67}$$

where M is the total number of elements in the solution domain. Assuming that the mesh has a total of N nodes, the energy function must be minimized with respect to each unknown in the solution domain. For the nth node potential V_n,

$$\boxed{\frac{\partial F(V)}{\partial V_n} = \sum_{m=1}^{M} \frac{\partial F_m}{\partial V_n} = 0} \tag{6.68}$$

This means that to minimize the energy function over the whole solution domain, we can minimize the energy function over each individual element separately and then add the results to obtain minimization over the global domain. Thus, the important point in establishing a numerical procedure of calculation is to obtain the generic term $\partial F_m/\partial V_n$ in the sum of **Eq. (6.68)**. This is done next.

Substituting the approximation for $\partial V/\partial x$ and $\partial V/\partial y$ from **Eq. (6.58)** into **Eq. (6.66)** and separating the integral over element m into two parts gives

$$F_m = \frac{\varepsilon}{2}\int_s \left[\left(\sum_{l=i,j,k}\frac{1}{2\Delta}q_l V_l\right)^2 + \left(\sum_{l=i,j,k}\frac{1}{2\Delta}r_l V_l\right)^2\right] ds - \rho\int_s \sum_{l=i,j,k} N_l V_l ds \tag{6.69}$$

In this relation, we also assumed ε and ρ are constant within element m and, therefore, were taken outside the integral signs. The first integral is due to the electric field intensity and will be evaluated first. Denoting the first integral in **Eq. (6.69)** as F_e and noting that neither q_l nor r_l depends on the coordinates x or y, the surface integral simply means multiplying the integrand by the surface of element i, which equals Δ. Thus, we can write

$$F_e = \frac{\varepsilon}{2}\int_s \left[\left(\sum_{l=i,j,k}\frac{1}{2\Delta}q_l V_l\right)^2 + \left(\sum_{l=i,j,k}\frac{1}{2\Delta}r_l V_l\right)^2\right] ds = \frac{\varepsilon\Delta}{2}\left[\left(\sum_{l=i,j,k}\frac{1}{2\Delta}q_l V_l\right)^2 + \left(\sum_{l=i,j,k}\frac{1}{2\Delta}r_l V_l\right)^2\right] \tag{6.70}$$

Expanding the sums

$$F_e = \frac{\varepsilon\Delta}{2}\left[\frac{1}{(2\Delta)^2}\left(q_i V_i + q_j V_j + q_k V_k\right)^2 + \frac{1}{(2\Delta)^2}\left(r_i V_i + r_j V_j + r_k V_k\right)^2\right] \tag{6.71}$$

Now, we are ready to calculate the second integral in **Eq. (6.69)**, which we denote as F_s:

$$F_s = \rho\int_s \sum_{l=i,j,k} N_l V_l ds \tag{6.72}$$

This is much more difficult to evaluate because the approximation for V depends both on x and on y [see **Eq. (6.57)**]. Instead of performing the integration, we note that the integral in **Eq. (6.72)** is proportional to the charge density ρ and potential V in the element as $F_s \propto \rho V\Delta$. An approximation to this quantity may be obtained assuming the voltage in the element to be the average between the three nodal potentials. Using this approximation, we get

$$F_s = \frac{\rho\Delta(V_1 + V_2 + V_3)}{3} \tag{6.73}$$

where the charge density ρ and the average potential are assumed to be at the centroid (center of gravity) of the element. Again, our reason for accepting this approximation is that as the size of elements decreases, the approximation becomes more accurate.

Now, the general expression of the energy function in a general finite element becomes

$$F_m = F_e - F_S = \frac{\varepsilon}{8\Delta}\left[\left(q_i V_i + q_j V_j + q_k V_k\right)^2 + \left(r_i V_i + r_j V_j + r_k V_k\right)^2\right] - \frac{\rho\Delta(V_1 + V_2 + V_3)}{3} \tag{6.74}$$

The minimization is completed by taking the derivative of the energy function with respect to each unknown potential value in element m:

$$\frac{\partial F_m}{\partial V_i} = \frac{\varepsilon}{4\Delta}\left[\left(q_i^2 V_i + q_i q_j V_j + q_i q_k V_k\right) + \left(r_i^2 V_i + r_i r_j V_j + r_i r_k V_k\right)\right] - \frac{\rho\Delta}{3} \tag{6.75}$$

$$\frac{\partial F_m}{\partial V_j} = \frac{\varepsilon}{4\Delta}\left[\left(q_j q_i V_i + q_j^2 V_j + q_j q_k V_k\right) + \left(r_j r_i V_i + r_j^2 V_j + r_j r_k V_k\right)\right] - \frac{\rho\Delta}{3} \tag{6.76}$$

$$\frac{\partial F_m}{\partial V_k} = \frac{\varepsilon}{4\Delta}\left[\left(q_k q_i V_i + q_k q_j V_j + q_k^2 V_k\right) + \left(r_k r_i V_i + r_k r_j V_j + r_k^2 V_k\right)\right] - \frac{\rho\Delta}{3} \tag{6.77}$$

Rewriting these three equations as a matrix gives

$$\begin{bmatrix} \partial F_m/\partial V_i \\ \partial F_m/\partial V_j \\ \partial F_m/\partial V_k \end{bmatrix} = \frac{\varepsilon}{4\Delta}\begin{bmatrix} q_i q_i + r_i r_i & q_i q_j + r_i r_j & q_i q_k + r_i r_k \\ q_j q_i + r_j r_i & q_j q_j + r_j r_j & q_j q_k + r_j r_k \\ q_k q_i + r_k r_i & q_k q_j + r_k r_j & q_k q_k + r_k r_k \end{bmatrix}\begin{bmatrix} V_i \\ V_j \\ V_k \end{bmatrix} - \frac{\rho\Delta}{3}\begin{bmatrix} 1 \\ 1 \\ 1 \end{bmatrix} \tag{6.78}$$

This is called an ***elemental matrix*** or an elemental contribution. We note the following:

(1) The matrix is symmetric ($a_{ij} = a_{ji}$). This is typical of most finite element formulations.
(2) For each element in the solution domain, we get a similar matrix. The differences are in the area Δ of the element and individual coefficients, but the form remains the same.
(3) The approximation for Laplace's equation is obtained by setting $\rho = 0$ in **Eq. (6.78)**.

6.5.2.4 Assembly of the Elemental Matrices

The next step is assembly of the elemental matrices into a ***global system*** of equations. The assembly is required because of the approach we took: that of minimizing the energy function in each element separately. The assembly is then the summation of all individual elemental matrices into the global matrix. To perform the summation, we create a large system of equations whose size is equal to the number of unknowns in the finite element discretized domain. To outline the method for matrix assembly, consider **Figure 6.31a**, where a small finite element mesh with four triangular elements and six nodes is shown. Note the element numbering (circled) and node numbering. The numbering of elements and nodes is arbitrary but must be sequential.

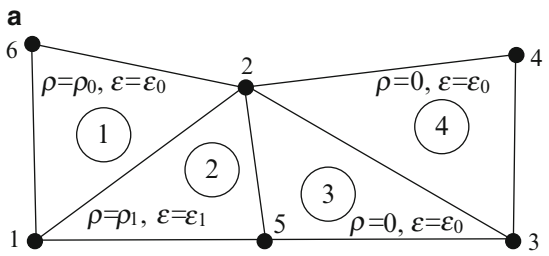

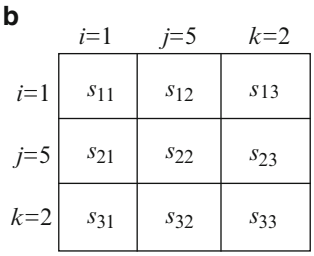

Figure 6.31 (**a**) A simple finite element mesh used to demonstrate matrix assembly. (**b**) The elemental matrix for element 2 in (**a**)

Figure 6.31b shows the form of the elemental matrix for element 2. The row and column numbers correspond to the node numbers of the corresponding element. The row and column numbers define the actual location in the global matrix. The coefficients of the elemental matrix in **Figure 6.31b** are entered in the global matrix as follows:
coefficient $s_{1,1}$ is added to coefficient $S_{1,1}$ in the global matrix
coefficient $s_{1,2}$ is added to coefficient $S_{1,5}$ in the global matrix
coefficient $s_{1,3}$ is added to coefficient $S_{1,2}$ in the global matrix
coefficient $s_{2,1}$ is added to coefficient $S_{5,1}$ in the global matrix
coefficient $s_{2,2}$ is added to coefficient $S_{5,5}$ in the global matrix
coefficient $s_{2,3}$ is added to coefficient $S_{5,2}$ in the global matrix
coefficient $s_{3,1}$ is added to coefficient $S_{2,1}$ in the global matrix
coefficient $s_{3,2}$ is added to coefficient $S_{2,5}$ in the global matrix
coefficient $s_{3,3}$ is added to coefficient $S_{2,2}$ in the global matrix

This process is repeated for all elements in the solution domain. In terms of the algorithm used for assembly, the normal practice is to generate an elemental matrix and immediately assemble it in the global matrix, before the next elemental matrix is assembled. We also note that an identical process applies to the right-hand side vector as well (elemental vectors q_i are assembled in global vector Q). After assembly, a global system of equations is obtained as

$$[S]\{V\} - \{Q\} = 0 \tag{6.79}$$

This system has six equations in six unknowns. Assembly of all four elements into the global system results in the following:

$$\begin{bmatrix} s_{11}^1+s_{11}^2 & s_{12}^1+s_{13}^2 & 0 & 0 & s_{12}^2 & s_{13}^1 \\ s_{31}^2+s_{21}^1 & s_{22}^1+s_{33}^2+s_{33}^3+s_{33}^4 & s_{32}^3+s_{31}^4 & s_{32}^4 & s_{32}^2+s_{31}^3 & s_{23}^1 \\ 0 & s_{23}^3+s_{13}^4 & s_{22}^3+s_{11}^4 & s_{12}^4 & s_{21}^3 & 0 \\ 0 & s_{23}^4 & s_{21}^4 & s_{22}^4 & 0 & 0 \\ s_{21}^2 & s_{23}^2+s_{13}^3 & s_{12}^3 & 0 & s_{22}^2+s_{11}^3 & 0 \\ s_{31}^1 & s_{32}^1 & 0 & 0 & 0 & s_{33}^1 \end{bmatrix} \begin{bmatrix} V_1 \\ V_2 \\ V_3 \\ V_4 \\ V_5 \\ V_6 \end{bmatrix} - \begin{bmatrix} (\rho_0\Delta_1)/3+(\rho_1\Delta_2)/3 \\ (\rho_0\Delta_1)/3+(\rho_1\Delta_2)/3 \\ 0 \\ 0 \\ (\rho_1\Delta_2)/3 \\ (\rho_0\Delta_1)/3 \end{bmatrix} = 0 \tag{6.80}$$

where the superscript indicates the element number from which the corresponding contribution was assembled.

6.5.2.5 Application of Boundary Conditions

As with any boundary value problem, we must apply boundary conditions to obtain a particular solution to the problem. In most cases, some of the nodes on the boundary of the problem are specified. These are then introduced into the matrix and the matrix is then reduced accordingly. For example, suppose the potentials at node 3 and node 6 are known and equal to V_0, their value is inserted in the matrix and the matrix reduced to a 4×4 matrix as follows:

$$\begin{bmatrix} s_{11}^1+s_{11}^2 & s_{12}^1+s_{13}^2 & 0 & s_{12}^2 \\ s_{31}^2+s_{21}^1 & s_{22}^1+s_{33}^2+s_{33}^3+s_{33}^4 & s_{32}^4 & s_{32}^2+s_{31}^3 \\ 0 & s_{23}^4 & s_{22}^4 & 0 \\ s_{21}^2 & s_{23}^2+s_{13}^3 & 0 & s_{22}^2+s_{11}^3 \end{bmatrix} \begin{bmatrix} V_1 \\ V_2 \\ V_4 \\ V_5 \end{bmatrix} - \begin{bmatrix} (\rho_0\Delta_1)/3+(\rho_1\Delta_2)/3-s_{13}^1\,V_0 \\ (\rho_0\Delta_1)/3+(\rho_1\Delta_2)/3-\left(s_{32}^3+s_{31}^4\right)V_0-s_{23}^1\,V_0 \\ -s_{21}^4\,V_0 \\ (\rho_1\Delta_2)/3-s_{12}^3\,V_0 \end{bmatrix} = 0 \tag{6.81}$$

This process is natural when only a few equations are involved or if the solution must be performed by hand. In finite element calculations, it is rather time-consuming, especially when the matrix is large. In addition, it has a big disadvantage in that the location of the unknowns is in the "wrong" places. For example, unknown potential V_5 is in location No. 4 in the solution vector. Every time we reduce the size of the matrix, we must keep track of the location of the unknowns. Again, in hand computation, this is a minor problem, but in a computer program, it is all too easy to lose track of the unknowns.

An alternative method is to leave the matrix unchanged but to force the unknowns V_3 and V_6 to be equal to the value V_0. This is done as follows:

(1) Replace the diagonal in the appropriate rows (row 3 and row 6) with a very large number P. This can be any convenient value, say $P = 10^{20}$.
(2) Replace the right-hand side by the known value V_0 multiplied by P (the right-hand side is now PV_0).

In effect, rows 3 and 6 have only a diagonal term and a right-hand side term because all other values in the row are negligible in comparison to P. For example, for row No. 3, we have

$$PV_3 - PV_0 = 0 \quad \rightarrow \quad V_3 = V_0$$

This method, although only approximate, is much more compatible with a computational method and is often used to impose boundary conditions in finite element applications.

So far, we discussed one type of boundary condition: specified potentials on the boundary. This type of boundary condition is called a ***Dirichlet boundary condition***. Another type of boundary condition is often useful in finite element calculations. It is called a ***Neumann boundary condition*** and occurs whenever the normal component of the electric field intensity in electrostatic applications is zero on a boundary. As an example of the types of boundary conditions applicable, consider the parallel plate capacitor shown in **Figure 6.32**. If the solution domain is the interior of the capacitor, then only the potentials on the two plates are required. These potentials are known and, therefore, are Dirichlet boundary conditions.

Now, suppose we cut the capacitor vertically in the middle on the line $A - A'$ and wish to solve for the potential on the right-hand side of the geometry. Line $A - A'$ becomes a boundary. This is permissible because we know the potential on the right-hand side is the same as that on the left-hand side of the boundary $A - A'$. The x component of the electric field intensity (normal to line $A - A'$) is zero. Thus, the boundary condition on line $A - A'$ is a Neumann boundary condition. Fortunately, in finite element applications, Neumann boundary conditions do not need to be specified. We simply leave the values on $A - A'$ unspecified. The Neumann boundary condition can be utilized every time we have a symmetry in the potentials in the problem. It is usually quite easy to identify symmetries. However, we must make sure that the normal component of the electric field intensity on any symmetry line is zero.

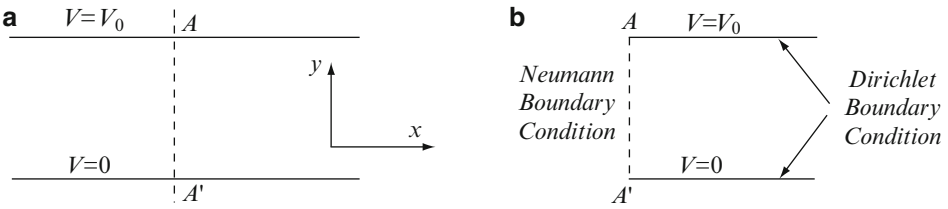

Figure 6.32 Boundary conditions in finite element applications. (**a**) Line $A - A' =$ is a geometric and potential symmetry line. (**b**) The upper and lower plates are Dirichlet boundary conditions. Line $A - A'$ is a Neumann boundary condition and is left unspecified

6.5.2.6 Solution

After applying boundary conditions, the system of equations is solved for the unknown values of V, as we shall see in examples. The solution of the system of equations can be performed using any applicable method. Gaussian elimination is often used for this purpose.

Example 6.8 Consider the problem shown in **Figure 6.33a**. It consists of an infinitely long enclosed, air-filled channel, with grounded sides ($V = 0$). The top is insulated from the sides and connected to a potential $V_0 = 100$ V. Calculate the potential distribution everywhere in the channel.

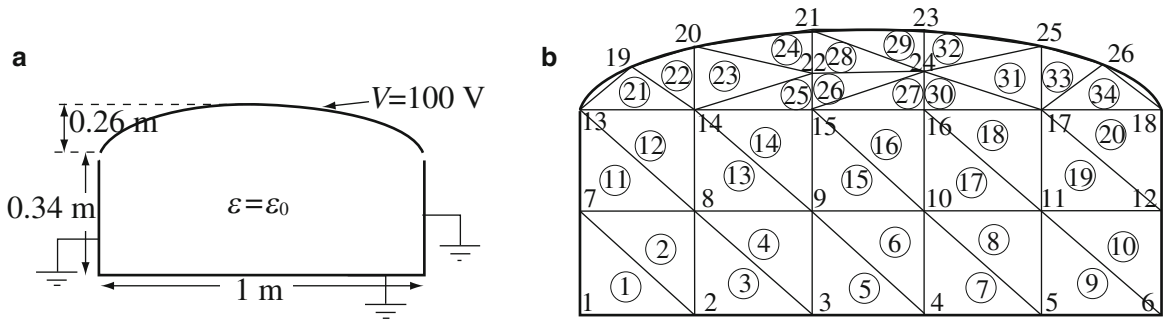

Figure 6.33 (**a**) Infinite channel (shown in cross section) with given boundary conditions. (**b**) Finite element mesh for the geometry in (**a**). Circled numbers are element numbers; the rest are node numbers

Solution: The steps involved in the solution are as follows:

(a) A finite element mesh must be defined. The mesh in **Figure 6.33b** is one choice which takes into account the shape of the geometry and uses a relatively small number of elements. A total of 34 elements and 26 nodes are used. Sixteen of the nodes are on the boundary and, therefore, are specified as Dirichlet boundary conditions. Nodes 1 through 6, 7, 12, 13, and 18 are set to zero, whereas nodes 19, 20, 21, 23, 25, and 26 are set to 100 V.

(b) The input data for the finite element program is defined from the mesh. This consists of the following:

(1) General mesh data. These include the number of nodes, number of elements, number of boundary conditions, and number of different materials in the geometry. The first record in **Figure 6.34** is the general mesh data for this example. The data, as used by the program, are listed in **dat2.**

(2) Element and material data. Each element is defined by three nodes and contains a single material. The element data consist of 34 records, one for each element, in the sequence they are numbered. Each line lists the three nodes of the element and a material index. Records 2 through 35 in **Figure 6.34** are the element data. The material index for all elements is 1 indicating that only one material is present (free space). Note also that the nodes of each element are numbered in a counterclockwise sequence.

(3) Node data. To calculate areas of elements, the coordinates of each node are needed. These are listed in sequence (coordinates of node 1, followed by node 2, and so on) as the next 26 records in the mesh data in **Figure 6.34**.

(4) Boundary and boundary condition data. The first line of the mesh data indicates how many boundary conditions are specified. In this case, there are two: one is zero, specified on the bottom and sides, and the second is 100 V, specified on the top. The boundary condition data are specified by entering the boundary condition value first, followed by the node numbers on which the value is specified. Thus, on line 62 **(Figure 6.34)**, the boundary condition 100.0 is specified. Line 63 gives 20 node numbers. The first six (19, 20, 21, 23, 25, and 26) are the nodes of the top boundary. The rest are zeros and are disregarded by the program. By entering a fixed number of boundary nodes, the data reading is simplified. Similarly, line 64 shows zero, followed by 20 node numbers on line 65. The first 10 are nodes on the bottom and side boundaries; the rest are disregarded.

Figure 6.34 Input mesh data for **Example 6.8.** * These lines were added for explanation purposes: they are not part of the data file

```
* General mesh data:
1     26 34 2 1
* Element data
2     1 2 7 1
3     2 8 7 1
4     2 3 8 1
5     3 9 8 1
6     3 4 9 1
7     4 10 9 1
8     4 5 10 1
9     5 11 10 1
10    5 6 11 1
11    6 12 11 1
12    7 8 13 1
13    8 14 13 1
14    8 9 14 1
15    9 15 14 1
16    9 10 15 1
17    10 16 15 1
18    10 11 16 1
19    11 17 16 1
20    11 12 17 1
21    12 18 17 1
22    13 14 19 1
23    14 20 19 1
24    14 22 20 1
25    22 21 20 1
26    14 15 22 1
27    15 24 22 1
28    15 16 24 1
29    22 24 21 1
30    24 23 21 1
31    16 17 24 1
32    24 17 25 1
33    24 25 23 1
34    17 26 25 1
35    17 18 26 1
* Node coordinates
36    0.0 0.0
37    0.2 0.0
38    0.4 0.0
39    0.6 0.0
40    0.8 0.0
41    1.0 0.0
42     0.0 0.16
43    0.2 0.16
44    0.4 0.16
45    0.6 0.16
46    0.8 0.16
47    1.0 0.16
48    0.0 0.34
49    0.2 0.34
50    0.4 0.34
51    0.6 0.34
52    0.8 0.34
53    1.0 0.34
54    0.05 0.46
55    0.2 0.55
56    0.4 0.6
57    0.4 0.46
58    0.6 0.6
59    0.6 0.46
60    0.8 0.55
61    0.95 0.46
* Boundary conditions
62    100.0
63    19 20 21 23 25 26 0 0
      0 0 0 0 0 0 0 0 0 0 0 0
64    0.0
65    1 2 3 4 5 6 7 12 13 18
      0 0 0 0 0 0 0 0 0 0
* Material properties
66    1.0 0.0
```

(5) Material data. For each material in the mesh, the relative permittivity is entered. In this case, the only material in the mesh is air and, therefore, line 66 lists as 1.0.

The input data are quite extensive although rather simple. In most finite element applications, these data are generated by special programs called mesh generators. The user only has to properly define the geometry of the problem and its properties. However, in this example and the examples that follow, the data may be entered by hand; this method is less exciting but does not require a mesh generator.

(c) Solution. Now that the mesh data are available (and, hopefully, correct), the finite element program is run to solve for the potentials at the nodes of the solution domain. Before doing so, the input data in **dat2** must be copied into a file named

dat1 which is used as the default input file for the finite element program. The program used here is called **fem1.m**. With the input data in **Figure 6.34**, the program produces the node potentials and electric field intensities and places these into two files. One is **out1** and lists the numerical output produced by the program. The second is **out2** and contains identical results as **out1** but with comments. The output produced with **dat2** is listed in **out2**. The potentials are calculated at the nodes and vary linearly within the element according to **Eq. (6.57)**. The electric field intensity as calculated here is averaged throughout each element and is associated with the centroid of the element. The listing produced by the program shows the x component, y component, and magnitude of the electric field intensity at the centroid of each element in the mesh.

(d) Postprocessing of data. The node potentials are rarely the only results needed. For example, we may wish to know the potential distribution in the solution domain. One way to see this is to show the contour plot (plot of constant potentials) as in **Figure 6.35**. Other types of results may be the energy per unit length stored in the geometry, potentials at points other than nodes, and many others.

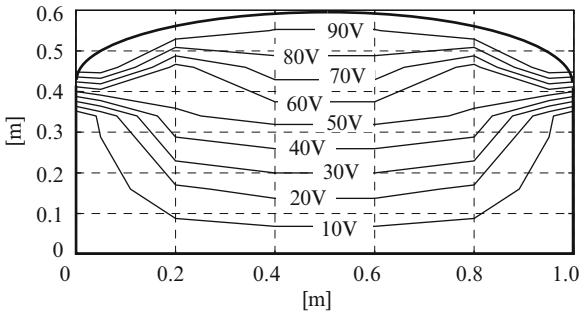

Figure 6.35 Plot of constant potential contours in the cross section of the channel in **Figure 6.33a**

Example 6.9 Application: Flaw in the Dielectric of a Capacitor A parallel plate capacitor is given. The insulation between the plates is mica with relative permittivity $\varepsilon_r = 4$. Because of problems in production, there is a fault in the mica in the form of a rectangular vein, as shown in **Figure 6.36**. The vain may be considered to be air:

(a) Calculate the potential everywhere inside the capacitor if a potential $V = 100$ V is connected across the plates.
(b) Calculate the electric field intensity at the center of the fault for the conditions in **(a)**.
(c) What is the maximum potential difference allowable with and without the fault if the dielectric strength in mica is 20×10^6 V/m, whereas in air it is 3×10^6 V/m?

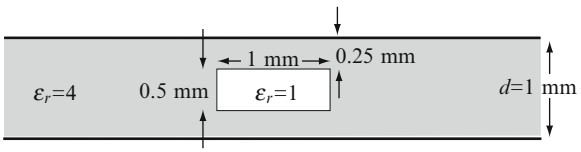

Figure 6.36 A mica insulated, parallel plate capacitor with a small flaw in the dielectric

Solution: The first step in the solution is to define a mesh. To do so, we note the following:

(1) The geometry in **Figure 6.36** is symmetric about a vertical line through the center of the flaw. Therefore, only half the geometry need be analyzed. We take the right-hand side.

(2) The capacitor is very large in relation to the distance d. In practice, we must analyze a finite-size geometry. Because the flaw is rather small, we expect any variation in the field to be around the flaw. Therefore, the right-hand side boundary is taken, arbitrarily, at 4 mm from the center of the flaw. The mesh with dimensions and boundary conditions is shown in **Figure 6.37**. The left side boundary is a symmetry line and, therefore, is a Neumann boundary. Nothing on this boundary need be specified. The top and bottom boundaries are Dirichlet boundaries since the potentials are known. The right boundary is an artificial boundary. It may be specified in one of two ways:

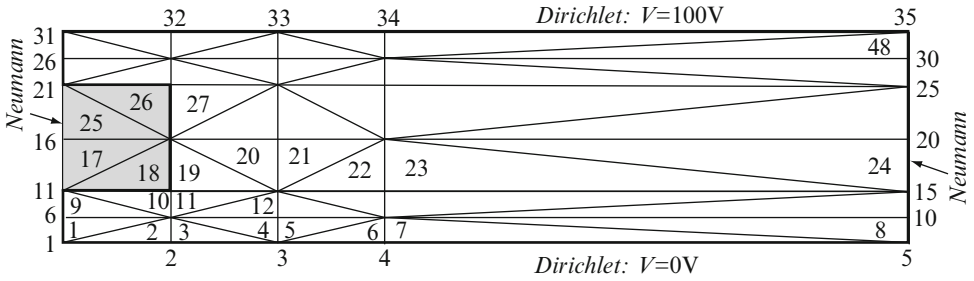

Figure 6.37 Finite element mesh and boundary conditions for the capacitor in **Figure 6.36**

(a) The potential at the boundary is the same as in an infinite capacitor (far enough from the flaw). Therefore, it is linearly distributed on the boundary. The potentials at nodes 10, 15, 20, 25, and 30 are 12.5 V, 25 V, 50 V, 75 V, and 87.5 V, respectively. These are Dirichlet boundary conditions. The total number of Dirichlet boundary conditions is seven: one on the top surface, one on the bottom, and five on the right-hand boundary.

(b) Alternatively, we may assume that the right boundary is also a Neumann boundary condition and leave it unspecified. This is justified by the fact that the normal electric field intensity at this boundary is zero, again, because the boundary is far from the defect. We choose this method here because it simplifies data input. With this, there are only two boundary conditions: one on the bottom boundary, one on the top. The top boundary is at 100 V (on nodes 31, 32, 33, 34, and 35) and the bottom boundary is at zero (on nodes 1, 2, 3, 4, and 5).

(a) The input data for the mesh are generated as in **Example 6.8**. and are listed in **dat3**. The solution is produced by first copying **dat3** into **dat1** (the input file specified in program **fem1.m**) and then running the program. The program produces output files **out1** and **out2**, as was described in **Example 6.8**. The output data (with comments) are listed in file **out3** (this is a copy of **out2**).
A contour plot of the potential is shown in **Figure 6.38a**.

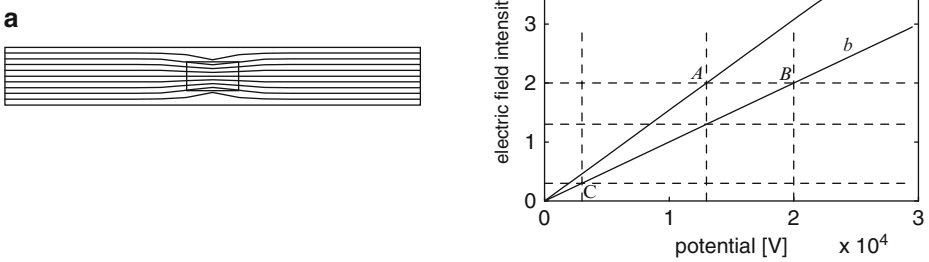

Figure 6.38 (**a**) Contours of constant potential in the capacitor in **Figure 6.36**. (**b**) Magnitude of the electric field intensity in the flaw as a function of applied potential

(b) The electric field intensity can only be calculated at the center of elements. There are four elements in the fault: elements 17, 18, 25, and 26. Of these, elements 17 and 25 are closest to the center of the fault. The electric field intensities at the center of these two elements are (from **out3**)

$$\mathbf{E}_{17} = \hat{\mathbf{x}}\, 7.629 \times 10^{-5} - \hat{\mathbf{y}}\, 1.539 \times 10^{2}, \quad \mathbf{E}_{25} = \hat{\mathbf{x}}\, 7.629 \times 10^{-5} - \hat{\mathbf{y}}\, 1.539 \times 10^{2} \quad \left[\frac{\mathrm{V}}{\mathrm{mm}}\right]$$

Taking the average between these two fields (which just happen to be the same) gives the approximate electric field intensity at the center of the flaw as

$$\mathbf{E}_{center} = \hat{\mathbf{x}}\, 7.629 \times 10^{-5} - \hat{\mathbf{y}}\, 1.539 \times 10^{2} \quad \left[\frac{\mathrm{V}}{\mathrm{mm}}\right]$$

Note that the field has a small x component and a dominant y component as expected.

(c) The maximum potential difference allowable without the flaw is calculated analytically as

$$V_{\max} = Ed = 20 \times 10^6 \times 0.001 = 20,000 \quad [\text{V}]$$

When the flaw is present, the potential is not uniformly distributed and we must calculate the potential difference numerically. However, there is a slight difficulty here: We are in effect trying to find the boundary conditions that will provide the maximum electric field intensity allowable in the flaw. The finite element method requires known boundary conditions to calculate the field intensity. The way we approach this problem is to start with a known potential difference and increment the potential on the boundary until the electric field intensity in the flaw (air) equals the breakdown electric field intensity. The potential difference thus obtained is the maximum allowable potential difference. In other words, we run the finite element program with known trial potentials and choose that potential which provides the required result. **Figure 6.38b** shows a plot of the magnitude of the electric field intensity in element 25 obtained for potential differences starting at 0 and ending at 20,000 V, in increments of 500 V. For each boundary potential value, the boundary conditions must be modified accordingly. From this figure, the maximum potential difference allowable is 13,000 V (point A). This is significantly lower than the 20,000 V (point B) allowed with an intact dielectric, but still much higher than about 3,000 V (point C) for an air-filled dielectric; that is, damage to the dielectric of the capacitor reduces its breakdown voltage significantly.

Example 6.10 Electric Fields Near a DC Busbar A busbar used in the distribution of electric power in a distribution box is at potential 220 V above ground. The busbar is a rectangular conductor as shown in **Figure 6.39a**. The ground and the busbar may be considered to be perfect conductors:

(a) Find the electric potential everywhere in space.
(b) Find the location and magnitude of the maximum electric field intensity.

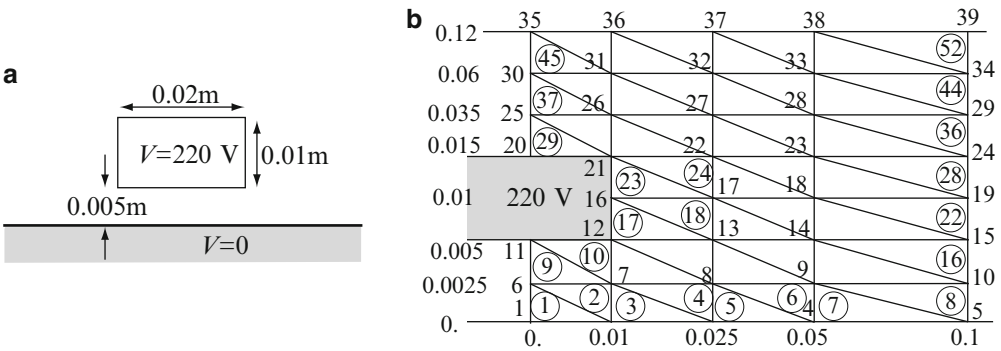

Figure 6.39 (**a**) A busbar at 220 V over a conducting ground. (**b**) Placement of artificial boundary and symmetry line for the geometry in (**a**). A mesh is also shown

Solution: We again start by defining the geometry and the boundary conditions. Using a symmetry line vertically through the center of the bar, we eliminate half the geometry. The cutting line becomes a Neumann boundary. Next, we must place artificial boundaries at some distance from the bar. By placing these boundaries at a reasonable distance from the source, the solution can be accurate while the mesh required is reasonably small. In this case, the boundaries are placed at 0.1 m from the symmetry line and 0.12 m from the ground plane, as shown in **Figure 6.39b**. These boundaries are chosen assuming their influence on the solution is minimal. If this turns out to be wrong, they will have to be taken further away. A total of 52 elements and 39 nodes are used. The left boundary is left unspecified with the exception of the bar which is held at 100 V.

(a) The mesh input data are again generated as in **Example 6.8** and are listed in **dat5.** This data file is now copied into **dat1** (default input file to the program) and program **fem1.m** is executed. The output appears in **out1** and **out2. out1** is used to plot the results and **out2**, which contains comments, is copied onto **out5**, which is also available. A contour plot of the potential is shown in **Figure 6.40**. Note that the results have been reflected about the symmetry line to show the potential everywhere.

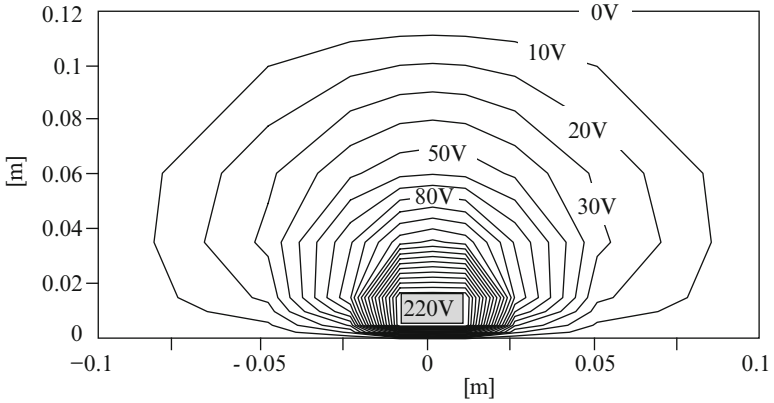

Figure 6.40 Contour plot of the solution for **Example 6.10**

(b) From the results in **out5**, the magnitude of the electric field intensity is highest in element No. 11 and equals 4.496×10^4 V/m. This value is calculated at the centroid of element No. 11 and corresponds to a distance of about 1.7 mm below and about 10 mm to the right of the corner of the busbar. That the maximum electric field must be around the corner is expected, but the exact location and magnitude depends on the dimensions and on the mesh used.

6.6 Summary

Numerical methods of solution are used when the analytical methods in **Chapters 3** through **5** fail, usually because the geometry is too complicated. The three methods described in this chapter are representative of the concepts involved.

The ***finite difference method*** replaces partial or ordinary derivatives with simple approximations. Given points x_i on a line, at distance $\Delta x = h$ from each other, with unknown values $f(x_i) = f_i$, the approximation to first- and second-order derivatives may be written as

$$\frac{df(x_i)}{dx} \approx \frac{f(x_i + \Delta x) - f(x_i - \Delta x)}{2\Delta x} = \frac{f_{i+1} - f_{i-1}}{2h} \tag{6.1}$$

$$\frac{d^2 f_i}{dx^2} \approx \frac{f_{i+1} - 2f_i + f_{i-1}}{h^2} \tag{6.8}$$

Similar expressions are written for derivatives with respect to y and z if needed. To use these approximations, the space in which a solution is sought is divided into a grid with points i,j, generated by parallel lines, separated distances $h = \Delta x = \Delta y$, in the two directions in space forming a two-dimensional grid (**Figure 6.5**). An unknown potential $V_{i,j}$, is assumed at each point of the grid and using the approximation in **Eq. (6.8)**, we get

$$V_{i,j} = \frac{V_{i-1,j} + V_{i+1,j} + V_{i,j-1} + V_{i,j+1}}{4} + h^2 \frac{\rho_{i,j}}{4\varepsilon_{i,j}} \tag{6.17}$$

This equation is repeated at each internal point of the grid. Boundary values are incorporated in the approximation when any of the values of $V_{i,j}$ corresponds to a boundary point. Solution of the system of equations provides the unknown values over the grid. Other quantities such as electric fields, forces, and energy can then be calculated from the potential. The extension to three dimensions is straightforward (see **Exercise 6.3**). The charge density at points of the grid can vary from point to point as can the permittivity.

The ***method of moments*** solves for the equivalent sources that produce a known potential. Given a charge distribution $\rho_{\Omega'}(x',y',z')$, the potential at a distance R from a differential point charge is

$$V(x,y,z) = \int_{\Omega'} \frac{1}{4\pi\varepsilon R} \rho_{\Omega'}(x',y',z') d\Omega' = \int_{\Omega'} K(x,y,z,x',y',z') \rho_{\Omega'}(x',y',z') d\Omega' \tag{6.23, 6.24}$$

$K(x,y,z,x',y',z')$ is a geometric function that depends on dimensions and permittivity and Ω' is the space in which the charge density is distributed (surface, volume). To apply the method, the space (say a plate) is divided into any number of subspaces (subsurfaces), an unknown charge density is assumed on each subsurface, and the potential on the surface must be known. The geometric function K is calculated for each pair of subsurfaces assuming the charge is concentrated at its center. Assuming the surface has been divided into N rectangular subsurfaces, each with an area $s_i = a_i \times b_i$, the known potential on subsurface j is

$$V_j = K_{jj}\rho_{sj} + \sum_{\substack{i=1 \\ i \neq j}}^{N} \rho_{si}K_{ij} \quad [\text{V}], \quad j = 1, 2, \ldots, N \tag{6.29}$$

where

$$K_{ij} = \frac{s_i}{4\pi\varepsilon\sqrt{\left(x_j - x_i'\right)^2 + \left(y_j - y_i'\right)^2 + \left(z_j - z_i'\right)^2}}, \quad i,j = 1, 2, \ldots, N, \quad i \neq j \tag{6.30}$$

$$K_{jj} = \frac{1}{4\pi\varepsilon}\left(2a_j \ln\frac{b_j + \sqrt{a_j^2 + b_j^2}}{a_j} + 2b_j \ln\frac{a_j + \sqrt{a_j^2 + b_j^2}}{b_j}\right) \tag{6.32}$$

Equation (6.29) is written for the potential on each subdomain to obtain N equations in N unknown values ρ_j. Solution of this system provides the charge density on each subdomain from which we can then calculate potentials and fields anywhere in space using the methods of **Chapters 3** and **4**.

Notes:

(1) The larger the number of subdomains, the more accurate the solution.
(2) Subdomains can be of different sizes or all equal in size.
(3) The potential must be known on each subdomain.
(4) When solving for the charge densities on plates of capacitors, the total charge on one plate must equal in magnitude to the total charge on the second. The potential of each plate must be adjusted to satisfy this condition (see **Example 6.7**).

The ***finite element method*** assumes the space (line, surface, volume) is divided into finite-size sections or elements and a potential distribution (constant, linear, quadratic, etc.) is assumed within each element based on the nodes (vertices) of the element. The potentials at these vertices are the unknowns we seek. The approximation for each element is then used to generate a system of equations for the unknown potentials. Given a triangular element with vertices (x_i,y_i), the potential within the element is

$$V(x, y) = N_i V_i + N_j V_j + N_k V_k \tag{6.43}$$

where N_i, N_j, N_k are called shape functions and V_i, V_j, V_k the unknown potentials at the nodes of the element. For a triangular element of area Δ and node coordinates (x_i, y_i), (x_j, y_j), and (x_k, y_k):

$$N_i = \frac{1}{2\Delta}\left[\left(x_j y_k - x_k y_j\right) + \left(y_j - y_k\right)x + \left(x_k - x_j\right)y\right] \tag{6.44}$$

$$N_j = \frac{1}{2\Delta}[(x_k y_i - x_i y_k) + (y_k - y_i)x + (x_i - x_k)y] \tag{6.45}$$

$$N_k = \frac{1}{2\Delta}\left[\left(x_i y_j - x_j y_i\right) + \left(y_i - y_j\right)x + \left(x_j - x_i\right)y\right] \tag{6.46}$$

To solve an electrostatic problem, we write the energy in a volume as

$$F(E) = \int_v \left(\frac{1}{2}\varepsilon E^2 - \rho V\right)dv \tag{6.63}$$

For the two-dimensional problems discussed in this chapter, assuming unit thickness for the geometry ($dv = 1ds$) and using $\mathbf{E} = -\nabla V$:

$$F(V) = \int_s \left(\frac{\varepsilon}{2} \left\{ \left(\frac{\partial V}{\partial x} \right)^2 + \left(\frac{\partial V}{\partial y} \right)^2 \right\} - \rho V \right) ds \tag{6.66}$$

This energy is minimized with respect to each unknown value in each element to produce a solution

$$\frac{\partial F(V)}{\partial V_n} = \sum_{m=1}^{M} \frac{\partial F_m}{\partial V_n} = 0 \tag{6.68}$$

M is the number of elements in the assembly (called a mesh) and N the number of nodes. **Equation (6.68)** produces N equations in N unknowns which, when boundary conditions are applied and the system solved, produces the potentials at the nodes of the finite element mesh.

The solution consists of the following:

(1) Definition of a finite element (triangle in two dimensions, tetrahedron in three dimensions, or any other defined shape that divides the space).
(2) Approximation of the potential over the element.
(3) The equation to solve is an energy related function [**Eq. (6.66)** for example].
(4) Minimization of the energy function over the space.
(5) Application of boundary conditions and solution for potentials.
(6) Electric fields can then be calculated from potentials if necessary (see **Example 6.10**).

Problems

Finite Differences

6.1 One-Dimensional Geometry. A parallel plate capacitor is shown in **Figure 6.41**. The capacitor may be viewed as infinite in extent. With $d = 1$ m and free space between the plates:

(a) Calculate the potential distribution everywhere within the capacitor using the finite difference method with four equal divisions.
(b) Repeat the solution in **(a)** with eight equal division.
(c) Calculate the potential distribution using direct integration. Show by comparison with **(a)** and **(b)** that the division does not matter in this case. Why?

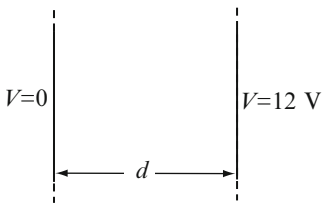

Figure 6.41

6.2 Application: Capacitor with Space Charge Between Plates. The parallel plate capacitor in **Figure 6.41** is given. In addition to the data in **Problem 6.1**, there is also a charge density everywhere inside the material such that $\rho/\varepsilon = 1$ C/F $\cdot$ m^2, where ρ is the charge density [C/m^3] and ε is the permittivity [F/m] of the dielectric between the plates:

(a) Find the potential distribution everywhere within the capacitor using four equal divisions.
(b) Repeat the solution in **(a)** with eight equal divisions. Show that the division chosen is important. Which division gives a better result? Compare with the analytical solution.

6.3 Capacitor with Space Charge. Consider the parallel plate capacitor in **Figure 6.42**. A uniform charge density $\rho_0 = 10^{-6}$ C/m^3 exists everywhere inside the capacitor and both plates are grounded. The permittivity of the material inside the capacitor equals $4\varepsilon_0$ [F/m]:

(a) Calculate the potential and electric field intensity everywhere inside the capacitor using a one-dimensional finite difference method.

(b) Find the analytic solution by direct integration and compare the numerical and analytic solutions.

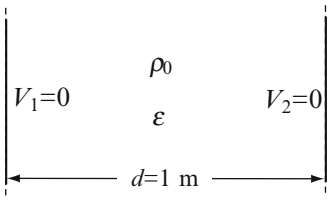

Figure 6.42

6.4 Infinite Channel. Solve for the electric potential in the geometry in **Figure 6.43**. This is a two-dimensional problem in the form of an infinite channel shown in cross section. The top conducting surface is physically separated from the side plates. Use an explicit method of solution.

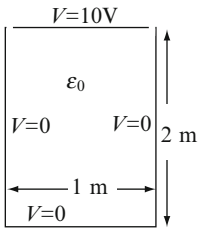

Figure 6.43

6.5 Infinite Channel with Interior Charge. Solve for the electric potential in the geometry given in **Figure 6.44**. The outer boundaries of the channel are grounded except for the top surface which is at 10 V and a charge distribution exists inside the channel as shown. Given: $\rho = 10^{-6}$ C/m^3, $\varepsilon_1 = 80\varepsilon_0$ [F/m].

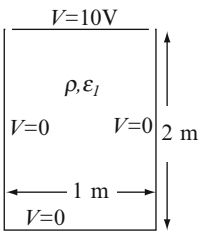

Figure 6.44

6.6 Infinite Channel with Interior Charge. Solve for the electric potential in the geometry in **Figure 6.45**. This is a two-dimensional problem similar to that in **Problem 6.4**, but the outer boundaries are grounded and a charge distribution exists inside part of the channel as shown. Given: $\rho = 10^{-6}$ C/m^3, $\varepsilon_1 = 80\varepsilon_0$ [F/m].

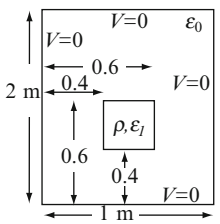

Figure 6.45

Method of Moments

6.7 Capacitance of Small Plates. Two rectangular plates are used as a variable capacitor by rotating one plate about the axis A–A while the other plate is fixed. In the two extremes, the plates are either parallel to each other or flat on a plane as shown in **Figures 6.46a** and **6.46b**. The plates are 50 mm by 20 mm in size. When parallel to each other, they are 2 mm apart, as shown in **Figure 6.46b**. When on a plane, they are separated 2 mm while the edges remain parallel. Calculate the range of the capacitor's capacitance.

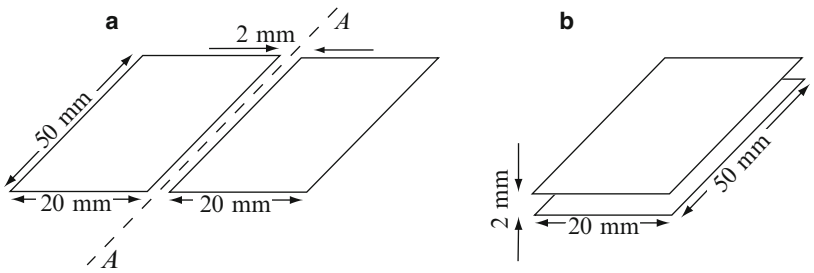

Figure 6.46

6.8 Application: Capacitance of a Ring. Calculate the capacitance of a thin, flat washer of internal radius $c = 10$ mm and external radius $d = 60$ mm.

6.9 Application: Small Capacitor. A parallel plate capacitor is made from two plates, as shown in **Figure 6.47a**. The material between the plates is free space:

(a) Calculate the capacitance of the capacitor.
(b) Now the capacitor is cut in two as shown in **Figure 6.47b**. Calculate the capacitance of one of the two smaller capacitors thus created. Is the sum of the capacitance of the two halves in **Figure 6.47b** equal to the capacitance of the whole capacitor in **Figure 6.47a**? If not, why not?

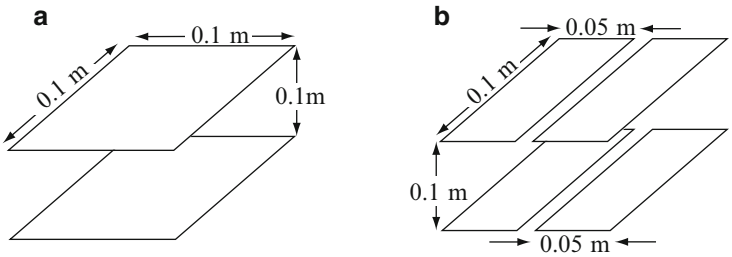

Figure 6.47

6.10 Application: Small Capacitor. Consider **Figure 6.47a**:

(a) Show by a series of calculations with increasing number of subdomains that as the number of subdomains increases, the capacitance of the small capacitor convergences to a constant value. What is this value?
(b) Plot the charge density on the upper plate on a line parallel to one of the sides of the plate and that crosses through the center of the plate (or very close to it). Comment on the shape of this plot and its meaning.

6.11 Application: Coupled-Charge Devices (CCD). In a memory array or a CCD (coupled-charge device), capacitive devices are arranged in a two-dimensional array. A 3×3 section is shown in **Figure 6.48**. The purpose of these capacitors is to store charge for a relatively short period of time. Each plate is 2 μm by 2 μm and the separation between two plates is 0.5 μm. As part of the analysis of the device, it is required to calculate the capacitances as follows (assume the plates are in free space):

(a) Between each two nearest plates (plates A and B).
(b) Between each plate and the plate on the diagonal (plates A and C).

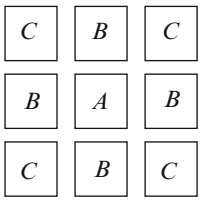

Figure 6.48

6.12 Capacitance of Perpendicular Plates. Two plates with given dimensions form a capacitor as shown in **Figure 6.49**. The plates are perpendicular to each other. With the dimensions given and assuming the plates are in air (free space):

- **(a)** Calculate the capacitance between the plates using the method of moments and hand computation. Use a small, reasonable number of subdomains.
- **(b)** If the potential difference between the plates is 1 V, what is the potential and the electric field intensity at point P? Use the charge densities obtained in **(a)** to calculate the potential at P.
- **(c)** Write a program (or use program **mom1.m**) to calculate a sequence of results, each with increasing number of subdomains until the change in solution is less than 5 %. What is the minimum number of subdomains needed if all subdomains must be of the same size?

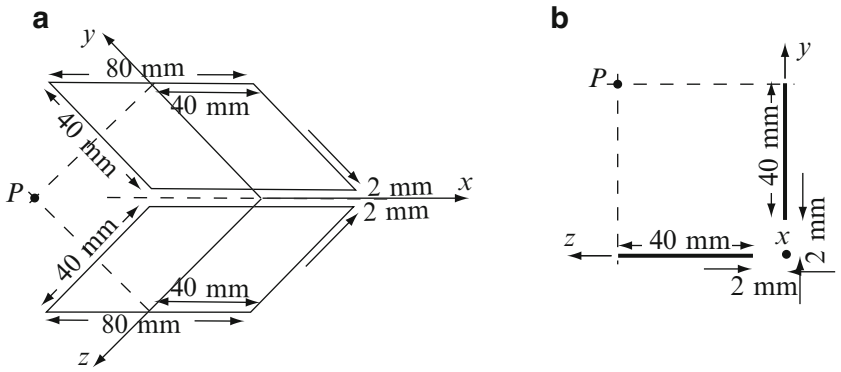

Figure 6.49

Finite Elements

6.13 One-Dimensional Finite Elements. A one-dimensional element may be defined in a manner similar to that in **Section 6.5.1.1** by assuming a section of a line of finite length, two points at its ends with coordinates (x_1) and (x_2), and unknown values ϕ_1 and ϕ_2 as shown in **Figure 6.50**:

- **(a)** For this element, calculate the shape functions necessary to define the element by assuming a linear variation inside the element of the form $\phi(x) = a + bx$.
- **(b)** With the shape functions in **(a)**, find an expression for the function $\phi(x)$ inside the element in terms of the shape functions.
- **(c)** Show that the magnitude of N_1 [shape function at node (1)] is 1 at node (1) and zero at node (2).
- **(d)** Show that the magnitude of N_2 [shape function at node (2)] is 1 at node (2) and zero at node (1).
- **(e)** Show that the sum of the shape functions at any point $x_1 \leq x \leq x_2$ equals 1.

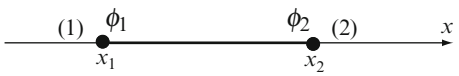

Figure 6.50

6.14 Field and Potential in Parallel Plate Capacitor. Consider the parallel plate capacitor with a dielectric between the plates shown in **Figure 6.51**. The dielectric has relative permittivity of 6 and a charge distribution as shown:

(a) Set up a finite element solution and solve for the potential, using the shape functions in **Problem 6.13**. Use hand computation and as many elements as necessary.
(b) From the potential distribution, calculate the electric field intensity in the capacitor. Sketch the solutions.
(c) Find the analytic solution for potential by direct integration and compare with the results in **(a)**.

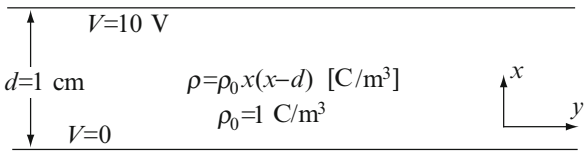

Figure 6.51

6.15 Field and Potential in Parallel Plate Capacitor. Consider **Figure 6.52**. Using the triangular shape functions defined in **Section 6.5.1** and the implementation in **Section 6.5.2**:

(a) Calculate the potential distribution inside the capacitor.
(b) From the potential distribution, calculate the electric field intensity in the capacitor. Sketch the solutions.
(c) Find the analytic solution and compare with **(a)** and **(b)**.

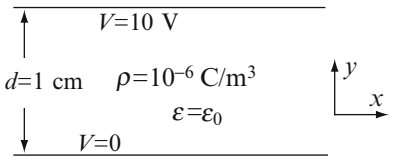

Figure 6.52

6.16 Quadrilateral Finite Elements. **Figure 6.53** shows a two-dimensional, four-node element (quadrilateral element). Assume an approximation of the form $\phi(x,y) = a + bx + cy + dxy$:

(a) Define the shape functions and their derivatives for a particular element with nodes at $P_1(0,0)$, $P_2(1,0)$, $P_3(1,1)$, and $P_4(0,1)$.
(b) Define the shape functions and their derivatives for the general element in **Figure 6.53**.
(c) Discuss the method and comment on its extension to more complex finite elements.

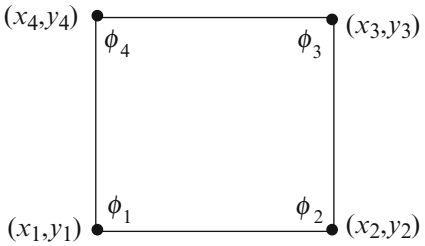

Figure 6.53

6.17 Application: Breakdown in Microcircuits. One of the challenges of microcircuits is the need for an ever-decreasing size of components. This means that components must be closer to each other and, therefore, the danger of breakdown between components and, in particular, between lines leading to them. To see the difficulty involved, consider the following: In a microcircuit, the smallest width conducting lines are 0.5 μm. Two such lines run side by side as shown in **Figure 6.54**. Assume the material below the lines is silicon with a relative permittivity of 12, and above and between the lines, it is free space. Breakdown in air occurs at 3×10^6 V/m and in silicon at 3×10^7 V/m. Assume the silicon layer is very thick:

(a) If the minimum distance between lines is $d = 0.5$ μm, what is the maximum potential difference allowable between the two lines? This is usually then taken as the maximum source voltage for the circuit.

(b) If the circuit must operate on a maximum potential difference of 5 V, what is the minimum distance allowed between the lines?

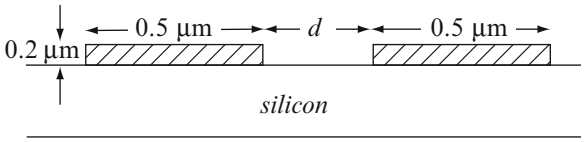

Figure 6.54

6.18 Application: Breakdown in Printed Circuits. The width of two strips on opposite sides of a printed circuit board is 1 mm and their thickness is 0.1 mm as shown in **Figure 6.55a**. The material is 0.5 mm thick, made of fiberglass with relative permittivity of 3.5. Breakdown voltage in fiberglass occurs at 30 kV/mm:

(a) What is the maximum potential difference allowable between the two strips?

(b) Suppose the printed circuit board has a flaw so that the material between the strips is missing, as shown in **Figure 6.55b**. What is now the maximum electric potential allowable?

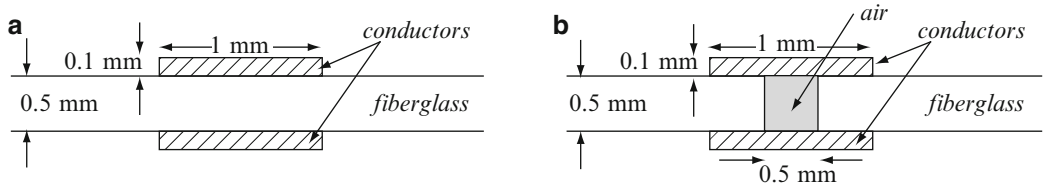

Figure 6.55

6.19 Application: Potential in Three-Phase Underground Cable. A three-phase power line operates at 240 V peak and is enclosed in a conducting shield which is at zero potential. The space between conductors and shield is filled with a material with relative permittivity 2.0:

(a) Assume the lines are very thin (**Figure 6.56a**) and calculate the potential distribution everywhere in the cable. Plot constant potential lines. The conditions are $r = 0.05$ m, $d = 0.01$ m, $V_1 = 240$ V, $V_2 = 240\cos(120°)$ [V], and $V_3 = 240\cos(240°)$ [V].

(b) The actual lines are each 10 mm in diameter (**Figure 6.56b**). Calculate the potential distribution everywhere in the cable. The conditions are $r = 0.05$ m, $d = 0.01$ m, $V_1 = 240$ V, $V_2 = 240\cos(120°)$ [V], and $V_3 = 240\cos(240°)$ [V]. **Hint**: The conductor surfaces become boundary conditions with known potentials. No need to discretize the interior of the conductors.

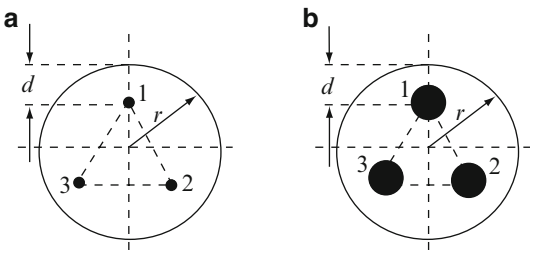

Figure 6.56